Chapter 2
Structural and Vibrational Study on Chromyl Acetate in Different Media

Abstract In this chapter, the structural and vibrational properties of chromyl acetate in different media were studied using density functional theory (DFT) methods. The initial geometries were fully optimized at different theory levels and the harmonic wavenumbers were evaluated at the same levels. Also, the characteristics and nature of the Cr–O and Cr ← O bonds for the stable structure were studied by means of the natural bond orbital (NBO) study while the topological properties of the electronic charge density were analyzed using the Bader atoms in the molecules theory (AIM). Besides, a complete assignment of all observed bands in the infrared spectrum for the compound was performed combining DFT calculations with Pulay′s scaled quantum mechanics force field (SQMFF) methodology.

Keywords Chromyl acetate · Vibrational spectra · Molecular structure · Force field · DFT calculations

2.1 Introduction

In organic chemistry, for a long time the chemical reactivity of chromyl acetate, $CrO_2(CH_3COO)_2$ was broadly studied because it is an effective reagent for the oxidation of numerous compounds, such as hydrocarbons [1, 2], olefins [3, 4], C-25 on cholestane side-chains to the corresponding C-25 hydroxy derivative [5], steroids [6] and indole alkaloids [7] among others, but so far their molecular structure is unknown. In a previous paper we could assign some of the observed bands in the infrared spectrum and for this their vibrational properties remain only partially characterized [8]. The study of compounds that contain chromyl groups [8–11] is interesting because depending of the ligand they can act with different

S. A. Brandán, *A Structural and Vibrational Investigation into Chromylazide, Acetate, Perchlorate, and Thiocyanate Compounds*, SpringerBriefs in Molecular Science,
DOI: 10.1007/978-94-007-5754-7_2,

coordination modes. In the chapter above, the structure and vibrational properties of the chromyl nitrate compound, $CrO_2(NO_3)_2$ were studied by means of the Density functional theory [10]. In this chapter, the geometries and the harmonic vibrational frequencies for chromyl acetate were evaluated at the B3LYP/Lanl2DZ, B3LYP/6-31G*, and B3LYP/6-311++G levels of theory. In this way, with the aid of calculations it was possible the assignment of all the observed bands in the vibrational spectra for the compound taking into account the type of coordination adopted by the acetate groups as monodentate and bidentate. In addition, as the nitrate group, the acetate group is an interesting ligand because it presents different coordination modes: monodentate or bidentate [8–23].

The properties of the $CrO_2(CH_3COO)_2$ compound prepared previously by us were completely different from the relatively volatile compound initially prepared according to *Krauss* [23, 24]. In this chapter a theoretical study of chromyl acetate, $CrO_2(CH_3COO)_2$, was performed in order to study the coordination mode of the acetate groups and carry out its complete assignment using the experimental spectra. The aim of this chapter is to carry out an experimental and theoretical study on this compound with the methods of quantum chemistry in order to have a better understanding of its vibrational properties. A precise knowledge of the normal modes of vibration is expected to provide a foundation for understanding the conformation-sensitive bands in vibrational spectra of this molecule. Here, the normal mode calculations were accomplished using a generalized valence force field (GVFF) and considering the acetate group as monodentate and bidentate ligands. For this purpose, the optimized geometry and frequencies for the normal modes of vibration were calculated first in gas phase and then in carbon tetrachloride (CCl_4) and dimethylsulfoxide (DMSO) solutions because the compound is soluble in all the inert organic solvents. In both cases, there are no publications about experimental or high-level theoretical studies on the geometries and force field of chromyl acetate. Hence, obtaining reliable parameters by theoretical methods is an appealing alternative. The parameters obtained may be used to gain chemical and vibrational insights into related compounds.

The election of the method and the basis sets are very important to evaluate, not only the best level of theory but also the best basis set to be used to reproduce the experimental geometry and the vibrational frequencies. In previous studies on Cr compounds, such as oxotetrachlorochromate (V) anion [25], it was found that the inclusion of polarization functions in the basis sets significantly improved the theoretical geometry results and the lowest deviation, with reference to the experimental data, was obtained for the 6-31G* and 6-311G* basis sets and the B3PW91 functional [25]. In this case the lower difference between theoretical and experimental frequencies, measured by the root mean standard deviation (RMSD), was obtained with the combination B3LYP/6-31+G. In the study of the structures and vibrational spectra of chromium oxo anions and oxyhalide compounds, Bell et al. [26] have found that the B3LYP/Lanl2DZ combination gives the best fit for the geometries and the observed vibrational spectra. However, in the chromyl nitrate case the results with the Lanl2DZ basis set were not satisfactory, for that reason here, that basis set was not considered. In this chapter, DFT calculations were used

to study the structure and vibrational properties of the compound. The normal mode calculations were accomplished using a GVFF. The molecular force field for the chromyl acetate, considering the acetate group as monodentate ligand calculated by using the DFT/6-31G* and 6-311++G** combinations is well represented. The force field produces satisfactory agreement between the calculated and experimental vibrational frequencies of chromyl acetate. DFT normal mode assignments, in terms of the potential energy distribution, are in general accord with those obtained from the normal coordinate analysis.

Also, the nature of the two types of Cr–O and Cr ← O bonds of chromyl acetate in gas phase and in both CCl_4 and DMSO solutions, were systematically and quantitatively investigated by the NBO analysis [27–29]. In addition, the topological properties of electronic charge density are analyzed using Bader atoms in molecules theory (AIM) [30].

2.2 Structural Study

The molecular structure for monodentate and bidentate chromyl acetate are shown in Fig. 2.1 together with the numbering of the atoms. The initial B3LYP structures modeled with different basis sets for chromyl acetate were carried out using C_2 symmetries according to the experimental structure obtained by Marsden et al. [11] for chromyl nitrate by using diffraction data and HF calculations. Table 2.1 shows a comparison of the total energies and dipole moment values for chromyl acetate with the B3LYP method using different basis sets.

In all cases, the most structure stable is obtained using the B3LYP/6-311++G** method combined with a diffuse function basis set, while the structure with higher energy is obtained using B3LYP/STO-3G calculation.

The structures were compared with those reported in the literature for barium and sodium acetate [31].

All the calculations in gas phase were made using the GAUSSIAN 03 [32] set of programs. The starting point for the geometry optimization was modeled with the *GaussView* program [33]. Calculations were made using hybrid density functional methods. In the last technique, Becke's three parameter functional and non-local correlation provided by Lee–Yang–Parr's (B3LYP) [34, 35] expressions were used, as implemented in the GAUSSIAN programs. Different basis sets were used. For the compound we realized the normal mode analysis using 6-31G* and 6-311++G** basis sets.

The harmonic force field in Cartesian coordinates for chromyl acetate which resulted from the calculations were transformed into "natural" internal coordinates [36] by the MOLVIB program [37, 38]. The natural coordinates for monodentate and bidentate chromyl acetates have been defined as proposed by Fogarasi et al. [39]. The analysis as bidentate ligand was performed with the two basis sets considering the acetate groups as two rings of four members where the deformations and torsion coordinates of these groups have been defined as proposed by Fogarasi et al. [39].

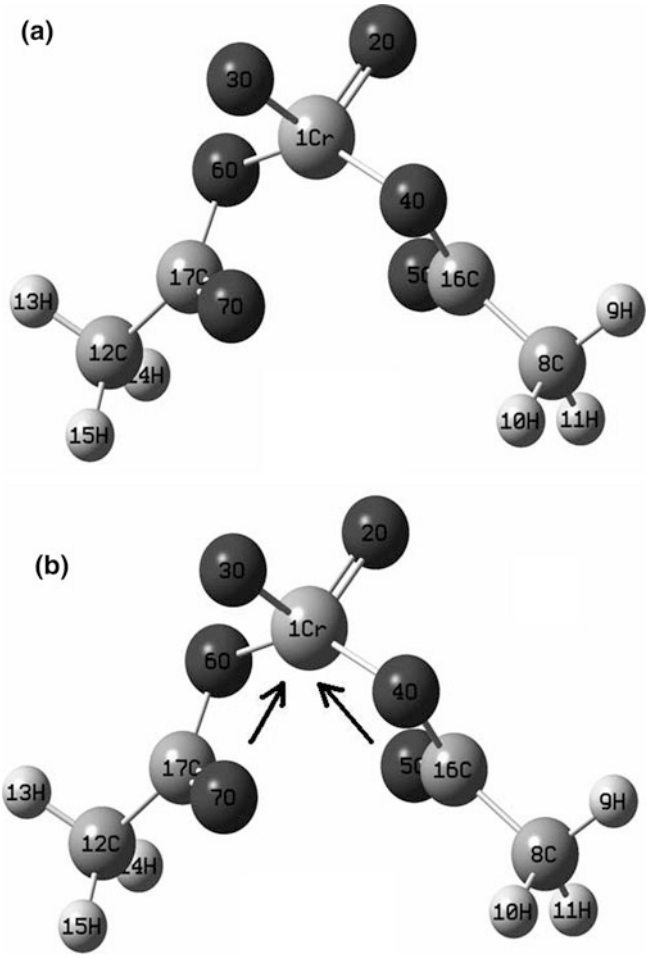

Fig. 2.1 The $C_2(1)$ molecular structure of chromyl acetate considering the acetate group as. **a** Monodentate ligand and **b** bidentate ligand

The numbering of the atoms for monodentate and bidentate chromyl acetates are described in Fig. 2.1

The scaled quantum mechanics (SQM) force field [40–42] was obtained using the transferable scale factors of Rauhut and Pulay [41] with the MOLVIB program [37, 38]. The potential energy distribution components (PED) larger than or equal to 10 % are subsequently calculated with the resulting SQM force field. The principal force constants for the compound were obtained.

An NBO analysis was then performed using the same basis sets with the NBO 3.1 program [43] included in GAUSSIAN 03 package programs [32]. The topological properties of the charge density in all systems studied were computed with the AIM2000 software [44].

Table 2.1 Total energy and dipole moment for chromyl acetate at B3LYP method

Basis set	ET (Hartree)	μ (D)
LANL2DZ	−693.68481616	3.09
STO-3G	−1633.03396705	2.47
3-21G*	−1643.67961761	3.27
6-31G	−1651.68610581	3.31
6-31G*	−1651.88702958	2.88
6-31+G	−1651.71932997	3.18
6-31+G*	−1651.91314474	2.81
6-311G*	−1652.10027672	2.54
6-311+G*	−1652.12267593	2.71
6-311++G**	−1652.13142696	2.73

The solvent effects were calculated with polarized continuum model (PCM) solvation model which were analyzed and compared with the obtained values in gas phase for the two studied basis sets. The use of an adequate basis set is important for the proper description of the solute–solvent interaction. Numerous authors have observed the dependency of the basis set on the SCRF calculated solvation [45, 46] and Pye et al. [47] have verified the greater changes induced adding diffuse function. Here, the B3LYP method using 6-31G* and 6-311++G** basis sets for SCRF calculations were used. To study the solvent effects the self-consistent reaction field method was employed. In this methodology, the solute molecule is located in a cavity surrounded by a continuum medium with a given dielectric constant. In this chapter, a value of 46.7 for the dielectric constant to simulate DMSO media and 2.228 for the dielectric constant to simulate CCl_4 media were used. In the simulation of the solvent effect, the self-consistent polarized continuum models have been used, as implemented in GAUSSIAN 03 and the cavity is created by a series of spheres, initially devised by Tomasi and Persico [48–50].

In addition, an NBO analysis for the two studied solvents were then performed with the NBO 3.1 program [43] using the 6-311++G** basis set and the topological properties of the charge density in two systems studied were computed with the AIM2000 software [44].

The dipole moment values do not follow a defined tendency as observed in Table 2.1. The calculation results with all basis sets used are given in Table 2.2.

The obtained theoretical parameters for the chromyl group were compared with the experimental values obtained for chromyl nitrate by Marsden et al. [11], while the calculated values for acetate group were compared with the recent experimental values obtained for acetate by Ibrahim et al. [51] and with those reported for sodium uranyl acetate [52], chromous acetate [53], sodium acetate [54], and anhydrous barium acetate [55]. In this way, the theoretical C–C and C–O bond distances are lower than the corresponding experimental values, while the C=O bond distance is longer than the observed value by Hsu et al. [54] for sodium acetate (1.245 Å).

Table 2.2 Comparison of calculated geometrical parameters at different levels of theory for chromyl acetate

B3LYP method

Atoms	STO-3G	3-21G*	6-31G	6-31G*	6-31+G	6-31+G*	6-311G*	6-311+G*	6-311++G**
Bond length (Å)									
(1,2)	1.484	1.563	1.576	1.551	1.579	1.557	1.549	1.554	1.554
(1,3)	1.484	1.563	1.576	1.551	1.579	1.557	1.549	1.554	1.554
(1,4)	1.859	1.875	1.925	1.913	1.920	1.913	1.909	1.916	1.917
(1,6)	1.859	1.875	1.925	1.913	1.920	1.913	1.909	1.916	1.917
(1,5)	2.169	2.330	2.323	2.261	2.343	2.276	2.286	2.293	2.292
(1,7)	2.169	2.330	2.323	2.261	2.343	2.276	2.286	2.293	2.292
(4,16)	1.356	1.351	1.342	1.30	1.344	1.310	1.306	1.307	1.307
(5,16)	1.302	1.259	1.269	1.245	1.268	1.246	1.238	1.239	1.239
(6,17)	1.356	1.351	1.342	1.309	1.344	1.310	1.306	1.307	1.307
(7,17)	1.302	1.259	1.269	1.245	1.268	1.246	1.238	1.239	1.239
(8,9)	1.102	1.094	1.094	1.095	1.090	1.095	1.092	1.092	1.092
(8,10)	1.102	1.095	1.096	1.095	1.090	1.096	1.093	1.092	1.093
(8,11)	1.100	1.089	1.090	1.091	1.091	1.091	1.088	1.088	1.088
(8,16)	1.544	1.490	1.485	1.497	1.486	1.497	1.495	1.494	1.494
(12,13)	1.102	1.094	1.094	1.095	1.095	1.095	1.092	1.092	1.092
(12,14)	1.102	1.095	1.096	1.095	1.096	1.096	1.093	1.093	1.093
(12,15)	1.100	1.089	1.090	1.091	1.091	1.091	1.088	1.088	1.088
(12,17)	1.544	1.490	1.486	1.497	1.486	1.497	1.495	1.494	1.494
Bond angle (°)									
(2,1,3)	107.5	107.1	108.1	107.9	108.3	108.2	107.9	108.2	108.2
(2,1,4)	101.9	103.5	103.7	104.0	103.9	104.3	103.8	104.2	104.2
(2,1,6)	98.1	99.9	98.6	97.9	98.7	97.9	98.3	98.2	98.1
(3,1,4)	98.1	99.9	98.6	979.208	98.7	97.9	98.3	98.2	98.1
(3,1,6)	101.9	103.5	103.7	104.0	103.9	104.3	103.8	104.2	104.2

(continued)

Table 2.2 (continued)

B3LYP method

Atoms	STO-3G	3-21G*	6-31G	6-31G*	6-31+G	6-31+G*	6-311G*	6-311+G*	6-311++G**
(4,1,6)	145.7	140.0	141.4	142.3	140.9	141.7	141.9	141.3	141.3
(1,4,16)	95.9	100.1	99.6	97.6	100.2	98.2	98.4	98.8	98.6
(1,6,17)	95.9	100.1	99.6	97.6	100.2	98.2	98.4	98.7	98.7
(9,8,10)	108.5	107.7	107.4	107.5	107.5	107.6	107.4	107.4	107.6
(9,8,11)	109.6	110.4	110.1	110.2	110.0	110.2	110.3	110.0	110.3
(9,8,16)	109.8	109.6	110.1	109.7	110.1	109.8	110.1	109.9	109.7
(10,8,11)	109.5	110.1	109.7	109.9	109.7	109.9	109.7	109.8	110.0
(10,8,16)	109.7	109.1	109.5	109.2	109.6	109.2	109.1	109.3	109.0
(11,8,16)	109.5	109.7	109.9	110.0	109.8	109.9	110.0	110.1	109.9
(13,12,14)	108.5	107.7	107.4	107.5	107.5	107.6	107.4	107.4	107.6
(13,12,15)	109.6	110.4	110.1	110.2	110.0	110.2	110.3	110.0	110.3
(13,12,17)	109.8	109.6	110.1	109.7	110.1	109.8	110.1	109.9	109.7
(14,12,15)	109.5	110.1	109.7	1.0	109.7	109.9	109.7	109.8	110.0
(14,12,17)	109.7	109.1	109.5	109.2	109.8	109.2	109.1	109.3	109.0
(15,12,17)	109.5	109.7	109.9	110.0	109.8	109.9	110.0	110.1	109.9
(4,16,5)	113.5	115.3	115.0	116.7	115.1	116.5	116.9	116.7	116.6
(4,16,8)	120.6	117.5	119.0	118.4	118.8	118.4	118.0	118.2	118.2
(5,16,8)	125.9	127.1	125.9	124.9	126.0	125.0	124.9	125.0	125.0
(6,17,7)	113.5	115.4	115.0	116.7	115.1	116.5	116.9	116.7	116.7
(6,17,12)	120.6	117.5	119.0	118.4.	118.8	118.4	118.0	118.2	118.2
(7,17,12)	125.9	127.1	125.9	124.9	126.0	125.0	124.9	125.0	125.0
Bond dihedral angle (°)									
(2,1,4,16)	−86.5	−86.2	−84.9	−83.8	−84.0	−83.3	−83.77	−83.5	−83.5
(3,1,4,16)	163.5	163.2	163.9	165.3	164.5	165.5	165.3	165.2	165.2
(6,1,4,16)	38.0	38.0	38.7	39.8	39.4	40.1	39.9	39.9	39.9

(continued)

Table 2.2 (continued)

B3LYP method

Atoms	STO-3G	3-21G*	6-31G	6-31G*	6-31+G	6-31+G*	6-311G*	6-311+G*	6-311++G**
(2,1,6,17)	163.5	163.2	163.9	165.3	164.5	165.5	165.3	165.2	165.2
(3,1,6,17)	−86.5	−86.2	−84.9	−83.8	−84.0	−83.3	−83.7	−83.5	−83.5
(4,1,6,17)	38.0	38.0	38.7	39.8	39.5	40.1	39.9	39.9	39.9
(1,4,16,5)	0.1	0.8	0.3	−0.5	−0.4	−0.6	−0.2	−0.4	−0.4
(1,4,16,8)	−178.9	−178.6	−179.0	−179.9	−179.9	179.8	−179.4	−180.0	−179.9
(1,6,17,7)	0.14	0.8	0.3	−0.5	−0.4	−0.6	−0.2	−0.4	−0.4
(1,6,17,12)	−178.9	−178.6	−179.0	−179.9	−179.9	179.8	−179.4	−180.0	−179.9
(9,8,16,4)	−58.3	−56.1	−54.6	−56.2	−55.5	−55.9	−52.6	−56.2	−55.6
(9,8,16,5)	122.7	124.4	126.2	124.3	124.9	124.4	128.2	124.2	124.8
(10,8,16,4)	60.8	61.6	63.3	615.294	62.5	17.713	65.0	61.5	62.0
(10,8,16,5)	−118.0	−117.8	−115.8	−117.9	−116.9	−117.8	−114.0	−118.0	−117.5
(11,8,16,4)	−178.8	−177.6	−176.1	−177.7	−176.9	−177.5	−174.5	−177.7	−177.2
(11,8,16,5)	22.6	29.5	46.9	28.4	35.9	29.3	63.6	27.1	32.6
(13,12,17,6)	−58.3	−56.1	−54.6	−56.1	−55.5	−55.9	−52.6	−56.2	−55.6
(13,12,17,7)	122.7	124.4	126.2	124.3	124.9	124.4	128.2	124.2	124.8
(14,12,17,6)	60.8	61.6	63.3	61.5	62.5	61.7	65.1	61.5	62.0
(14,12,17,7)	−118.0	−117.8	−115.8	−117.9	−116.9	−117.8	−114.0	−118.0	−117.5
(15,12,17,6)	−178.8	−177.6	−176.1	−177.6	−176.8	−177.5	−174.5	−177.7	−177.2
(15,12,17,7)	22.6	29.5	46.9	28.4	35.9	29.3	63.6	27.1	32.6

The calculated O–C–O bond angles with all the methods used are lower than the corresponding experimental values, while the O–C–C bond angles are longer than the reported values of 118 ° for sodium acetate [54]. According to these results, the method and basis set that best reproduces the experimental parameters for the chromyl acetate compound is B3LYP/6-31+G*, where the mean difference for bond lengths is 0.029 Å, while with B3LYP/3-21G* it is 4.1° for angles. The B3LYP functional gives somewhat less satisfactory agreement using the STO-3G (0.06 Å and 5.0°) and 6-31G (0.034 Å and 4.6°) basis sets. The inclusion of polarization functions, however, is important to have a better agreement with the experimental geometry: mean differences degrade to 0.031 Å and 4.34° for the 6-311++G** basis set. Similar to the experimental structure of chromyl nitrate [11], also with B3LYP calculations, we can represent the coordination around Cr as derived from a severely distorted octahedron where the acetate groups act as bidentate ligands and are asymmetrically bonded to Cr. The bond orders, expressed by Wiberg's indexes for chromyl acetate are given in Tables 2.3 and 2.4 and are compared with the values obtained for chromyl nitrate [10]. In this compound the chromium atom forms six bonds using 6-311++G** basis sets, two Cr=O bonds (bond order 1.9582), two Cr–O (bond order 0.5502), and two Cr ← O (bond order 0.1837). In chromyl nitrate the bonds order of these bonds are quite similar by using 6-311+G basis set, they are: two Cr=O (bond order 1.9721), two Cr–O (bond order 0.5374), and two Cr ← O (bond order 0.1821). The bond order value of this last bond was estimated by Marsden et al. [11] between 0.19 and 0.29, while for chromyl acetate it is slightly bigger than chromyl nitrate. Theoretically, in the B3LYP calculations the Cr–O–COO angle values are practically planar with the Cr atom with a variation of the dihedral angle between 0.1 and 0.8°, as can be seen in Table 2.2. In addition, in chromyl nitrate using B3LYP calculations and ab initio method, Marsden et al. [11] predict that the O=Cr=O bond angle in chromyl nitrate is smaller than the O–Cr–O angle, in contradiction with the valence-shell electron-pair (VSEPR) theory [56, 57]. In chromyl acetate a similar observation is found. This fact was explained on the basis of the delocalized and/or bonding characters of the relevant molecular orbitals (MO), as observed in the series of the $VO_2X_2^-$ anions [58] and chromyl nitrate [10]. The atomic orbital coefficients (AO) for Cr atom of chromyl acetate (d-type orbitals) using 6-31G * and 6-311++G** basis sets are observed in Table 2.5. For the chromyl acetate the strongest bonding MOs involving Cr d-type orbitals that seem to be sensitive to the geometry can be considered, in increasing energy, those numbered as 20 (HOMO-36), 21 (HOMO-36) and 22 (HOMO-37) calculated with 6-31G* basis set, while those numbered as 25 (HOMO-52), 25 (HOMO-54) and 25 (HOMO-54) calculated with 6-311++G** basis set tend to widen the O_4–Cr_1–O_8 angle (125.3° by using 6-31G* basis set) on a maximum overlapping basis.

Table 2.3 Wiberg bond index matrix of chromyl acetate at different levels of theory

	Atoms	B3LYP method								
		6-31G* basis set								
		1	2	3	4	5	6	7	8	9
1.	Cr	0.0000	1.9419	1.9419	0.5180	0.1771	0.5180	0.1771	0.0219	0.0004
2.	O	1.9419	0.0000	0.2311	0.0728	0.0153	0.0650	0.0569	0.0038	0.0003
3.	O	1.9419	0.2311	0.0000	0.0650	0.0569	0.0728	0.0153	0.0017	0.0003
4.	O	0.5180	0.0728	0.0650	0.0000	0.1524	0.0247	0.0075	0.0208	0.0032
5.	O	0.1771	0.0153	0.0569	0.1524	0.0000	0.0075	0.0035	0.0364	0.0143
6.	O	0.5180	0.0650	0.0728	0.0247	0.0075	0.0000	0.1524	0.0005	0.0000
7.	O	0.1771	0.0569	0.0153	0.0075	0.0035	0.1524	0.0000	0.0003	0.0000
8.	C	0.0219	0.0038	0.0017	0.0208	0.0364	0.0005	0.0003	0.0000	0.9013
9.	H	0.0004	0.0003	0.0003	0.0032	0.0143	0.0000	0.0000	0.9013	0.0000
10.	H	0.0005	0.0003	0.0001	0.0035	0.0149	0.0001	0.0003	0.8976	0.0013
11.	H	0.0024	0.0002	0.0004	0.0073	0.0020	0.0002	0.0001	0.9129	0.0007
12.	C	0.0219	0.0017	0.0038	0.0005	0.0003	0.0208	0.0364	0.0000	0.0000
13.	H	0.0004	0.0003	0.0003	0.0000	0.0000	0.0032	0.0143	0.0000	0.0000
14.	H	0.0005	0.0001	0.0003	0.0001	0.0003	0.0035	0.0149	0.0000	0.0000
15.	H	0.0024	0.0004	0.0002	0.0002	0.0001	0.0073	0.0020	0.0000	0.0000
16.	C	0.0122	0.0078	0.0065	1.2133	1.5431	0.0014	0.0031	1.0192	0.0066
17.	C	0.0122	0.0065	0.0078	0.0014	0.0031	1.2133	1.5431	0.0002	0.0000

	Atoms	10	11	12	13	14	15	16	17
1.	Cr	0.0005	0.0024	0.0219	0.0004	0.0005	0.0024	0.0122	0.0122
2.	O	0.0003	0.0002	0.0017	0.0003	0.0001	0.0004	0.0078	0.0065
3.	O	0.0001	0.0004	0.0038	0.0003	0.0003	0.0002	0.0065	0.0078
4.	O	0.0035	0.0073	0.0005	0.0000	0.0001	0.0002	1.2133	0.0014
5.	O	0.0149	0.0020	0.0003	0.0000	0.0003	0.0001	1.5431	0.0031
6.	O	0.0001	0.0002	0.0208	0.0032	0.0035	0.0073	0.0014	1.2133

(continued)

Table 2.3 (continued)

	Atoms	10	11	12	13	14	15	16	17
7.	O	0.0003	0.0001	0.0364	0.0143	0.0149	0.0020	0.0031	1.5431
8.	C	0.8976	0.9129	0.0000	0.0000	0.0000	0.0000	1.0192	0.0002
9.	H	0.0013	0.0007	0.0000	0.0000	0.0000	0.0000	0.0066	0.0000
10.	H	0.0000	0.0008	0.0000	0.0000	0.0000	0.0000	0.0074	0.0001
11.	H	0.0008	0.0000	0.0000	0.0000	0.0000	0.0000	0.0041	0.0000
12.	C	0.0000	0.0000	0.0000	0.9013	0.8976	0.9129	0.0002	1.0192
13.	H	0.0000	0.0000	0.9013	0.0000	0.0013	0.0007	0.0000	0.0066
14.	H	0.0000	0.0000	0.8976	0.0013	0.0000	0.0008	0.0001	0.0074
15.	H	0.0000	0.0000	0.9129	0.0007	0.0008	0.0000	0.0000	0.0041
16.	C	0.0074	0.0041	0.0002	0.0000	0.0001	0.0000	0.0000	0.0007
17.	C	0.0001	0.0000	1.0192	0.0066	0.0074	0.0041	0.0007	0.0000

	B3LYP method								
	6-311++G** basis set								
	Atoms	1	2	3	4	5	6	7	8	9
1.	Cr	0.0000	1.9582	1.9582	0.5502	0.1837	0.5502	0.1837	0.0246	0.0005
2.	O	1.9582	0.0000	0.2815	0.0898	0.0157	0.0693	0.0704	0.0049	0.0004
3.	O	1.9582	0.2815	0.0000	0.0693	0.0704	0.0898	0.0157	0.0030	0.0003
4.	O	0.5502	0.0898	0.0693	0.0000	0.1536	0.0374	0.0083	0.0209	0.0035
5.	O	0.1837	0.0157	0.0704	0.1536	0.0000	0.0083	0.0034	0.0368	0.0146
6.	O	0.5502	0.0693	0.0898	0.0374	0.0083	0.0000	0.1536	0.0006	0.0000
7.	O	0.1837	0.0704	0.0157	0.0083	0.0034	0.1536	0.0000	0.0005	0.0000
8.	C	0.0246	0.0049	0.0030	0.0209	0.0368	0.0006	0.0005	0.0000	0.9166
9.	H	0.0005	0.0004	0.0003	0.0035	0.0146	0.0000	0.0000	0.9166	0.0000
10.	H	0.0008	0.0003	0.0002	0.0039	0.0152	0.0001	0.0003	0.9123	0.0014
11.	H	0.0029	0.0003	0.0006	0.0069	0.0019	0.0002	0.0001	0.9296	0.0007
12.	C	0.0246	0.0030	0.0049	0.0006	0.0005	0.0209	0.0368	0.0000	0.0000

(continued)

Table 2.3 (continued)

	B3LYP method								
	6-311++G** basis set								
	Atoms	1	2	3	4	5	6	7	8	9
13.	H	0.0005	0.0003	0.0004	0.0000	0.0000	0.0035	0.0146	0.0000	0.0000
14.	H	0.0008	0.0002	0.0003	0.0001	0.0003	0.0039	0.0152	0.0000	0.0000
15.	H	0.0029	0.0006	0.0003	0.0002	0.0001	0.0069	0.0019	0.0000	0.0000
16.	C	0.0160	0.0124	0.0114	1.1993	1.5531	0.0022	0.0026	1.0162	0.0072
17.	C	0.0160	0.0114	0.0124	0.0022	0.0026	1.1993	1.5531	0.0003	0.0000

	Atoms	10	11	12	13	14	15	16	17
1.	Cr	0.0008	0.0029	0.0246	0.0005	0.0008	0.0029	0.0160	0.0160
2.	O	0.0003	0.0003	0.0030	0.0003	0.0002	0.0006	0.0124	0.0114
3.	O	0.0002	0.0006	0.0049	0.0004	0.0003	0.0003	0.0114	0.0124
4.	O	0.0039	0.0069	0.0006	0.0000	0.0001	0.0002	1.1993	0.0022
5.	O	0.0152	0.0019	0.0005	0.0000	0.0003	0.0001	1.5531	0.0026
6.	O	0.0001	0.0002	0.0209	0.0035	0.0039	0.0069	0.0022	1.1993
7.	O	0.0003	0.0001	0.0368	0.0146	0.0152	0.0019	0.0026	1.5531
8.	C	0.9123	0.9296	0.0000	0.0000	0.0000	0.0000	1.0162	0.0003
9.	H	0.0014	0.0007	0.0000	0.0000	0.0000	0.0000	0.0072	0.0000
10.	H	0.0000	0.0008	0.0000	0.0000	0.0000	0.0000	0.0082	0.0001
11.	H	0.0008	0.0000	0.0000	0.0000	0.0000	0.0000	0.0040	0.0000
12.	C	0.0000	0.0000	0.0000	0.9166	0.9123	0.9296	0.0003	1.0162
13.	H	0.0000	0.0000	0.9166	0.0000	0.0014	0.0007	0.0000	0.0072
14.	H	0.0000	0.0000	0.9123	0.0014	0.0000	0.0008	0.0001	0.0082
15.	H	0.0000	0.0000	0.9296	0.0007	0.0008	0.0000	0.0000	0.0040
16.	C	0.0082	0.0040	0.0003	0.0000	0.0001	0.0000	0.0000	0.0008
17.	C	0.0001	0.0000	1.0162	0.0072	0.0082	0.0040	0.0008	0.0000

Table 2.4 Wiberg index and atomic charges of chromyl acetate at different levels of theory

Atoms	Numbers	6-31G*		6-311++G**	
		Atomic charges	Wiberg index	Atomic charges	Wiberg index
Cr	1	1.55826	5.3488	1.21848	5.4736
O	2	−0.34082	2.4044	−0.23001	2.5186
O	3	−0.34082	2.4044	−0.23001	2.5186
O	4	−0.64091	2.0905	−0.60230	2.1464
O	5	−0.65241	2.0272	−0.62687	2.0600
O	6	−0.64091	2.0905	−0.60230	2.1464
O	7	−0.65241	2.0272	−0.62687	2.0600
C	8	−0.77846	3.8167	−0.66706	3.8663
H	9	0.26943	0.9285	0.23782	0.9452
H	10	0.27229	0.9269	0.24133	0.9435
H	11	0.26468	0.9312	0.23204	0.9479
C	12	−0.77846	3.8167	−0.66706	3.8663
H	13	0.26943	0.9285	0.23782	0.9452
H	14	0.27229	0.9269	0.24133	0.9435
H	15	0.26468	0.9312	0.23204	0.9479
C	16	0.82706	3.8259	0.80581	3.8337
C	17	0.82706	3.8259	0.80581	3.8337

2.3 Calculations in Solution

Total (E) and solvation energies (ΔG) and dipole moment for chromyl acetate in CCl_4 and DMSO solutions are observed in Table 2.6 at B3LYP/6-31G* and B3LYP/6-311++G** levels of theory.

On the other hand, a comparison of the theoretical geometrical parameters in gas phase with the obtained values in solutions is observed in Table 2.7 The more stable structure in solution, the greater solvation energy values, and the lower dipole moment values using the two basis sets are obtained for the compound in DMSO solvent.

This behavior could be related probably to the partially ionic nature of the compound and then will explain the affinity of the solvent for the polar compound. In solution, the more important change in the geometrical parameters are observed in the distances where the Cr_1–O_5 and Cr_1–O_7 bond lengths are about 0.95 Å lower than the corresponding values in gas phase. Moreover, the variations are independent of the solvent because in the two cases considered the values are approximately the same. This observation is probably explained due to strong association of the molecules in solution media. Also, when the compound is solvated in the CCl_4 or DMSO solvents, the C–H bond lengths of the two acetate groups undergo a slight increase in approximately 0.4 Å and, as a consequence of the solvent effect, the C_8–C_{16} bond length decreases more strongly (0.402 Å) than the C_{12}–C_{17} distance. For this reason, the dihedral angles involved in the changes also undergo variations between 3.4 and 6.4°, as observed in Table 2.7.

Table 2.5 Atomic orbital coefficients (AO) for Cr atom of chromyl acetate at B3LYP level

6-31G*				6-311++G**			
N° orbital	Type orbital	HOMO-36	HOMO-37	N° orbital	Type orbital	HOMO-36	HOMO-37
18	6XX	−0.33178	0.00000	25	15D 0	0.15892	0.00000
19	6YY	0.07504	0.00000	26	15D+1	0.00000	0.21345
20	6ZZ	0.24774	0.00000	27	15D−1	0.00000	−0.11802
21	6XY	0.18994	0.00000	28	15D+2	−0.13523	0.00000
22	6XZ	0.00000	0.35911	29	15D−2	0.11457	0.00000
23	6YZ	0.00000	−0.19411	30	16D 0	0.16165	0.00000
24	7XX	−0.20429	0.00000	31	16D+1	0.00000	0.22423
25	7YY	0.04488	0.00000	32	16D−1	0.00000	−0.12192
26	7ZZ	0.16284	0.00000	33	16D+2	−0.14011	0.00000
27	7XY	0.11686	0.00000	34	16D−2	0.11908	0.00000
28	7XZ	0.00000	0.20458	35	17D 0	0.15837	0.00000
29	7YZ	0.00000	−0.11549	36	17D+1	0.00000	0.20227
30	8F0	0.01138	0.00000	37	17D−1	0.00000	−0.11466
31	8F+1	0.00000	0.00858	38	17D+2	−0.12927	0.00000
32	8F−1	0.00000	−0.00403	39	17D−2	0.10925	0.00000
33	8F+2	0.00416	0.00000	40	18S	−0.00120	0.00000
34	8F−2	0.00292	0.00000	41	19PX	0.00000	0.02540
35	8F+3	0.00000	−0.00043	42	19PY	0.00000	0.04889
36	8F-3	0.00000	−0.00425	43	19PZ	0.06290	0.00000
				44	20PX	0.00000	−0.00099
				45	20PY	0.00000	0.00879
				46	20PZ	0.04372	0.00000
				47	21D 0	0.05593	0.00000
				48	21D+1	0.00000	0.00350
				49	21D-1	0.00000	−0.00900
				50	21D+2	0.01428	0.00000
				51	21D-2	−0.01112	0.00000

Table 2.6 Total (E) and solvation energies (ΔG) and dipole moment for chromyl acetate in different solvents

Solvents	B3LYP/PCM method					
	E (Hartree)		ΔG (Kcal/mol)		μ (D)	
	6-31G*	6-311++G**	6-31G*	6-311++G**	6-31G*	6-311++G**
DMSO	−1651.886	−1652.131	−6.93	−7.52	3.06	2.90
CCl_4	−1651.882	−1652.125	−2.83	−3.02	3.23	3.20

2.4 Topological Study

For chromyl acetate the intermolecular interactions have been analyzed using Bader′s topological analysis of the charge electron density, ρ(r) by means of the AIM program [44]. The localization of the critical points in the ρ(r) and the values

Table 2.7 Comparison of theoretical geometrical parameters in gas phase and in CCl_4 and DMSO solutions at different levels of theory for chromyl acetate

[a]B3LYP method

	Gas Phase		CCl_4		DMSO	
Atoms	6-31G*	6-311++G**	6-31G*	6-311++G**	6-31G*	6-311++G**
Bond length (Å)						
(1,2)	1.551	1.554	1.553	1.555	1.554	1.555
(1,3)	1.551	1.554	1.553	1.555	1.554	1.555
(1,4)	1.913	1.917	1.912	1.916	1.912	1.915
(1,6)	1.913	1.917	1.912	1.916	1.912	1.915
(1,5)	2.261	2.292	1.310	1.308	1.311	1.308
(1,7)	2.261	2.292	1.247	1.241	1.248	1.240
(4,16)	1.300	1.307	1.310	1.308	1.311	1.308
(5,16)	1.245	1.239	1.247	1.241	1.248	1.240
(6,17)	1.309	1.307	1.095	1.092	1.095	1.092
(7,17)	1.245	1.239	1.095	1.093	1.096	1.093
(8,9)	1.095	1.092	1.091	1.088	1.091	1.088
(8,10)	1.095	1.093	1.495	1.491	1.492	1.491
(8,11)	1.091	1.088	1.095	1.092	1.095	1.092
(8,16)	1.497	1.494	1.095	1.093	1.096	1.093
(12,13)	1.095	1.092	1.091	1.088	1.091	1.088
(12,14)	1.095	1.093	1.495	1.491	1.492	1.491
(12,15)	1.091	1.088	1.553	1.555	1.554	1.555
(12,17)	1.497	1.494	1.553	1.555	1.554	1.555
Bond angle (°)						
(2,1,3)	107.9	108.2	108.0	108.3	108.1	108.2
(2,1,4)	104.0	104.2	104.2	104.5	104.6	104.4
(2,1,6)	97.9	98.1	97.6	97.9	97.2	97.9
(3,1,4)	97.9	98.1	97.6	97.9	97.2	97.9

(continued)

Table 2.7 (continued)

[a]B3LYP method

	Gas Phase		CCl_4		DMSO	
Atoms	6-31G*	6-311++G**	6-31G*	6-311++G**	6-31G*	6-311++G**
(3,1,6)	104.0	104.2	104.2	104.5	104.6	104.4
(4,1,6)	142.3	141.3	142.4	141.4	142.4	141.5
(1,4,16)	97.6	98.6	97.6	98.7	97.5	98.7
(1,6,17)	97.6	98.7	97.6	98.7	97.5	98.7
(9,8,10)	107.5	107.6	107.6	107.6	107.6	107.7
(9,8,11)	110.2	110.3	110.2	110.4	110.2	110.3
(9,8,16)	109.7	109.7	109.7	109.6	109.6	109.6
(10,8,11)	109.9	110.0	110.0	110.0	109.9	110.0
(10,8,16)	109.2	109.0	109.2	109.0	109.2	109.0
(11,8,16)	110.0	109.9	110.0	110.0	110.1	110.0
(13,12,14)	107.5	107.6	107.6	107.6	107.6	107.7
(13,12,15)	110.2	110.3	110.2	110.4	110.2	110.3
(13,12,17)	109.7	109.7	109.7	109.6	109.6	109.6
(14,12,15)	110.0	110.0	110.0	110.0	109.9	110.0
(14,12,17)	109.2	109.0	109.2	109.0	109.2	109.0
(15,12,17)	110.0	109.9	110.0	110.0	110.1	110.0
(4,16,5)	116.7	116.6	116.2	116.2	115.7	116.2
(4,16,8)	118.4	118.2	118.6	118.5	118.9	118.5
(5,16,8)	124.9	125.0	125.1	125.3	125.4	125.3
(6,17,7)	116.7	116.7	116.2	116.2	115.7	116.2
(6,17,12)	118.4	118.2	118.6	118.5	118.9	118.5
(7,17,12)	124.9	125.0	125.1	125.3	125.4	125.3

(continued)

Table 2.7 (continued)

[a]B3LYP method

	Gas Phase		CCl_4		DMSO	
Atoms	6-31G*	6-311++G**	6-31G*	6-311++G**	6-31G*	6-311++G**
Bond dihedral angle (°)						
(2,1,4,16)	−83.8	−83.5	−83.4	−83.1	−82.9	−83.0
(3,1,4,16)	165.3	165.2	166.0	166.0	166.2	165.7
(6,1,4,16)	39.8	39.9	40.2	40.3	40.6	40.4
(2,1,6,17)	165.3	165.2	166.0	166.0	166.2	165.7
(3,1,6,17)	−83.8	−83.5	−83.4	−83.1	−82.9	−83.1
(4,1,6,17)	39.8	39.9	40.2	40.3	40.6	40.4
(1,4,16,5)	−0.5	−0.4	−0.7	−0.6	−0.8	−0.7
(1,4,16,8)	−179.9	−179.9	179.7	179.8	179.6	179.6
(1,6,17,7)	−0.5	−0.4	−0.7	−0.6	−0.8	−0.7
(1,6,17,12)	−179.9	−179.9	179.7	179.8	179.6	179.6
(9,8,16,4)	−56.2	−55.6	−56.8	−56.1	−56.5	−56.4
(9,8,16,5)	124.3	124.8	123.6	124.3	124.0	123.9
(10,8,16,4)	61.5	62.0	60.9	61.5	61.1	61.2
(10,8,16,5)	−117.9	−117.5	−118.6	−118.0	−118.3	−118.4
(11,8,16,4)	−177.7	−177.2	−178.2	−177.7	−178.0	−177.9
(11,8,16,5)	28.4	32.6	22.0	27.3	24.9	24.2
(13,12,17,6)	−56.1	−55.6	−56.8	−56.1	−56.5	−56.4
(13,12,17 ,7)	124.3	124.8	123.6	124.3	124.0	123.9
(14,12,17,6)	61.5	62.0	60.9	61.5	61.1	61.2
(14,12,17,7)	−117.9	−117.5	−118.6	−118.0	−118.3	−118.4
(15,12,17,6)	−177.6	−177.2	−178.2	−177.7	−178.0	−177.9
(15,12,17,7)	28.4	32.6	22.0	27.3	25.0	24.2

[a] This work

Table 2.8 Analysis of bond critical points in chromyl acetate compared with chromyl nitrate

Chromyl nitrate						
B3LYP/6-311++G						
Bond	Cr_1–O_4	$Cr_1 \leftarrow O_6$	Cr_1–O_8	$Cr_1 \leftarrow O_{10}$	(3, +1)	(3, +1)
ρ(r)	0.379166	0.301963	0.379166	0.301963	0.0374596	0.0374596
$\nabla^2\rho$(r)	**−0.186240**	0.043910	**−0.186240**	0.043910	0.015960	0.015960
$\lambda 1$	−0.919694	−0.700007	−0.919694	−0.700007	−0.0342722	−0.0342722
$\lambda 2$	−0.852381	−0.641803	−0.852381	−0.641803	0.0578309	0.0578309
$\lambda 3$	1.585836	1.385788	1.585836	1.385788	0.1360750	0.1360750
$\lvert\lambda 1\rvert/\lambda 3$	0.57990	0.505200	0.57990	0.505200	0.250620	0.250620
Chromyl acetate						
B3LYP/6−311++G**						
Bond	Cr_1–O_4	$Cr_1 \leftarrow O_5$	Cr_1–O_6	$Cr_1 \leftarrow O_7$	(3, +1)	(3, +1)
ρ(r)	0.11650	0.04979	0.11650	0.04386	0.04029	0.04029
$\nabla^2\rho$(r)	**0.38672**	0.17678	**0.38357**	0.17678	0.18192	0.18180
$\lambda 1$	−0.22187	−0.05126	−0.22241	−0.05136	−0.04241	−0.04242
$\lambda 2$	−0.20548	−0.03874	−0.20727	−0.03891	0.05268	0.05275
$\lambda 3$	0.81409	0.26679	0.81326	0.26677	0.17164	0.17147
$\lvert\lambda 1\rvert/\lambda 3$	0.27254	0.19213	0.27348	0.19252	0.24708	0.24739
(Chromyl acetate in CCl_4) PCM/B3LYP/6-311++G**						
Bond	Cr_1–O_4	$Cr_1 \leftarrow O_5$	Cr_1–O_6	$Cr_1 \leftarrow O_7$	(3, +1)	(3, +1)
ρ(r)	0.12971	0.039726	0.12971	0.03972	0.03776	0.03776
$\nabla^2\rho$(r)	**0.42561**	0.16205	**0.42240**	0.16183	0.16827	0.16814
$\lambda 1$	−0.25742	−0.04403	−0.25790	−0.04413	−0.03845	−0.03849
$\lambda 2$	−0.23598	−0.02945	−0.23778	−0.02956	0.03930	0.03934
$\lambda 3$	0.91902	0.23554	0.91809	0.23552	0.16744	0.16729
$\lvert\lambda 1\rvert/\lambda 3$	0.28010	0.18693	0.28090	0.18737	0.22963	0.23007
(Chromyl acetate in DMSO) PCM/B3LYP/6-311++G**						
Bond	Cr_1–O_4	$Cr_1 \leftarrow O_5$	Cr_1–O_6	$Cr_1 \leftarrow O_7$	(3, +1)	(3, +1)
ρ(r)	0.11650	0.04386	0.11650	0.04386	0.04029	0.04029
$\nabla^2\rho$(r)	**0.38672**	0.17678	**0.38357**	0.17648	0.18192	0.18180
$\lambda 1$	−0.22187	−0.05126	−0.22241	−0.05136	−0.04241	−0.04242
$\lambda 2$	−0.20548	−0.03874	−0.20727	−0.03891	0.05268	0.05275
$\lambda 3$	0.81409	0.26679	0.81326	0.26677	0.17165	0.17148
$\lvert\lambda 1\rvert/\lambda 3$	0.27253	0.19213	0.27347	0.19252	0.24707	0.24737

The quantities are in atomic units

of the Laplacian at these points are important for the characterization of molecular electronic structure in terms of interactions nature and magnitude. In this study the results using 6-311++G** basis set were compared with those obtained for chromyl nitrate using 6-311++G basis set [10] and can be seen in Table 2.8 The analyses of the Cr ← O bonds' critical points for the compound studied are

reported as well in gas phase as in solution calculations. In one case, the $Cr_1 \leftarrow O_5$ and $Cr_1 \leftarrow O_7$ bonds' critical points have the typical properties of the closed-shell interaction. That is, the values of $\rho(r)$ are relatively low (0.05 and 0.3 a.u.) as in chromyl nitrate while the $Cr_1 \leftarrow O_6$ and $Cr_1 \leftarrow O_{10}$ bonds' critical points, the relationship, $|\lambda 1|/\lambda 3$ are < 1 and the Laplacian of the electron density, $\nabla^2\rho(r)$ (0.04 and 0.2 a.u.), are positive indicating that the interaction is dominated by the contraction of charge away from the interatomic surface toward each nucleus [59–66]. The other important observation is related to the topological properties of the $Cr_1 \leftarrow O_4$ and $Cr_1 \leftarrow O_6$ bonds' critical points as shown in Table 2.8. In these cases, the electron density values are aproximately 0.1 a.u. while the positive values of the Laplacian of the electron density for the Cr ← O bonds (0.4 a.u.), as observed in Table 2.8, indicate that the $Cr_1 \leftarrow O_4$ and $Cr_1 \leftarrow O_6$ bonds' critical points are found in a region of charge depletion. The interaction $Cr_1 \leftarrow O_4$ bond is the same as the $Cr_1 \leftarrow O_6$ bond, which has no characteristic of the shared interaction, i.e., the value of electron density at the bond critical point is relatively high and the Laplacian of the charge density is positive indicating that the electronic charge is not concentrated in the internuclear region. These values of the Laplacian of the charge density do not agree with the values obtained for the $Cr_1 \leftarrow O_4$ and $Cr_1 \leftarrow O_8$ bonds in chromyl nitrate as can be seen in Table 2.8 [10]. The two last bonds in that compound are more covalently bonded than Cr_1–O_4 and Cr_1–O_6 in chromyl acetate. The different topological property values of the two Cr ← O bonds for chromyl acetate are not in agreement with those above B3LYP level results analyzed for chromyl nitrate. Evidently the nature of both compounds is different between them.

The $\rho(r)$ and $\nabla^2\rho(r)$ at the critical points related to Cr ← O bonds are not comparable with the respective 0.395 and 1.164 a.u. values reported for the Cr–O bond critical point in the $CrOF_4$ compound [57]. The $\rho(r)$ and $\nabla^2\rho(r)$ at the critical points related to the Cr_1–O_4 and Cr_1–O_6 bonds are comparable with the respective 0.091 and 0.429 a.u. values reported for the Cr–F_{eq} bond critical point in the $CrO_2F_4^{2-}$(cis) compound [57]. Moreover, the (3, +1) critical point as shown in Table 2.8 in chromyl acetate would confirm the nature of the two Cr ← O bonds in the respective structure. The two ring points of the electron density obtained by AIM analysis reveals that the mode of coordination adopted for the acetate groups in chromyl acetate is monodentate. These results indicated that the character of Cr ← O bonds are different in chromyl acetate from the nitrate compound in spite of the theoretical structure supporting the conclusions about the nature of the coordination of the Cr atom for this compound being similar to that observed by electron-diffraction experiments in gas phase in chromyl nitrate [10]. For the $Cr_1 \leftarrow O_5$ and $Cr_1 \leftarrow O_7$ bonds the values of $\rho(r) < 0.07$ a.u. are characteristic of ionic closed-shell interactions, while for the Cr_1–O_4 and Cr_1–O_6 bonds the large values of $\rho(r)$ are indicative of a strong shared interaction and, moreover, the slightly large positive values of $\nabla^2\rho(r)$ indicate a polar displacement toward oxygen consistent with the view that the MO bonds are strong polar simple bonds [57] different from the $Cr{=}O_2$ and $Cr{=}O_3$ bonds where large positive values of

ρ(r) (0.303 a.u.) and $\nabla^2\rho$(r) (0.996 a.u.) indicate a polar displacement toward oxygen consistent with strong polar double bonds [57].

2.5 Vibrational Study

The infrared spectra of the solid chromyl acetate in a KBr pellet and in d_6-DMSO solutions were taken from a previous study where the compound was obtained as reported in Ref. [24] and from our measurements [8]. The mentioned spectra were compared with the vibrational spectra of barium and sodium acetate obtained from the literature [31]. The structure for the compound has C_2 symmetry and 45 vibrational normal modes including 23 A + 22 B modes. All vibrational modes are infrared and Raman active. Table 2.9 shows the calculated harmonic frequencies for chromyl acetate using B3LYP method with different basis sets. Note that the lowest theoretical frequencies were not observed in the infrared spectrum and, for this reason, the lower frequencies of barium acetate were taken as experimental values. In all cases, the theoretical values were compared with the respective experimental values by means of the RMSD values. It can be seen that the best results are obtained with a B3LYP/6-311++G** calculation and that the introduction of diffuse functions (but not of polarization functions!) is essential to have a good approximation of the experimental values, especially in the case of the Cr=O and Cr–O stretchings. The calculated harmonic frequencies for chromyl acetate in CCl_4 and DMSO solvents using two basis sets are observed in Table 2.10. The important shiftings are observed in DMSO in relation to CCl_4 solvent and more specially related to bands associated with the observed change in the distances mentioned in the section corresponding to structural analysis. This analysis was performed taking into account both possibilities for acetate groups: monodentate and bidentate because it is impossible to differentiate between them on grounds of infrared and Raman spectra alone [7, 10, 17]. The observed frequencies and the assignment for chromyl acetate considering the coordination adopted by acetate groups as monodentate and bidentate are given in Table 2.11.

Vibrational assignments were made on the basis of the potential energy distributions (PED) in terms of symmetry coordinates and by comparison with molecules that contain similar groups [5, 7–17].

We will refer to the results obtained at B3LYP level with 6-31G* basis set because after scaling this method a satisfactory agreement is obtained between the calculated and the experimental vibrational frequencies of chromyl acetate. In general, the theoretical Infrared spectrum of chromyl acetate demonstrates good agreement with the experimental spectrum (see Fig. 2.2). Below, we discuss the assignment of the most important groups for the compounds studied considering the two coordination kinds.

Table 2.9 Calculated harmonic frequencies (cm^{-1}) for chromyl acetate using B3LYP method with different basis sets

STO-3G	3-21G*	6-31G	6-31+G	6-31+G*	6-31G*	6-311G*	6-311+G*	6-311++G**
3495	3183	3188	3181	3175	3182	3160	3158	3154
3495	3183	3188	3181	3175	3182	3160	3158	3154
3472	3130	3140	3135	3133	3139	3119	3117	3114
3472	3130	3140	3135	3133	3139	3119	3117	3114
3313	3074	3070	3066	3069	3074	3057	3056	3051
3313	3074	3070	3066	3069	3074	3057	3056	3051
1677	1609	1593	1577	1655	1670	1660	1647	1645
1676	1602	1585	1571	1650	1664	1654	1641	1639
1643	1534	1510	1506	1492	1497	1486	1485	1471
1643	1534	1510	1506	1492	1497	1486	1485	1470
1623	1516	1500	1494	1485	1491	1481	1479	1464
1622	1514	1499	1492	1484	1490	1480	1478	1463
1535	1451	1450	1445	1436	1444	1427	1423	1415
1535	1451	1450	1445	1434	1441	1425	1422	1413
1477	1313	1350	1328	1384	1392	1374	1368	1364
1464	1297	1338	1318	1377	1385	1366	1360	1356
1424	1158	1101	1099	1088	1110	1103	1084	1084
1415	1134	1101	1099	1086	1109	1102	1081	1078
1120	1107	1081	1067	1080	1092	1079	1078	1071
1120	1107	1065	1054	1078	1089	1079	1074	1070
1073	1036	1038	1034	1026	1029	1024	1022	1017
1073	1034	1036	1033	1026	1028	1024	1022	1016
952	907	929	923	959	963	961	959	958
949	900	923	917	955	958	956	954	954
741	727	706	707	719	720	724	719	719
715	726	701	702	713	713	716	713	713
579	602	600	607	614	611	617	619	617
555	602	597	603	611	608	614	615	614
555	545	519	518	523	523	528	522	522
537	531	506	506	512	513	519	512	512
508	449	434	426	446	454	457	445	446
414	385	382	379	382	384	387	381	381
379	325	319	315	323	327	326	320	320
333	287	280	279	282	284	290	281	281
317	280	263	258	262	266	268	260	260
267	230	223	218	229	233	235	227	228
254	208	202	191	202	210	203	199	199
252	169	168	158	182	193	181	176	177
240	158	163	158	176	181	178	172	172
164	141	141	136	148	148	150	146	146
115	109	101	98	102	105	104	100	100
109	92	77	74	76	87	80	74	74
84	76	57	56	72	78	76	63	63
57	69	57	56	50	53	56	46	46
56	48	33	−33	50	52	55	45	45

Table 2.10 Calculated harmonic frequencies (cm^{-1}) for chromyl acetate in CCl_4 and DMSO solvents using B3LYP method with different basis sets

Gas		DMSO		CCl_4	
		PCM	PCM	PCM	PCM
6-31G*	6-311++G**	6-31G*	6-311++G**	6-31G*	6-311++G**
3182	3154	3178	3149	3191	3141
3182	3154	3178	3149	3191	3141
3139	3114	3131	3105	3138	3091
3139	3114	3131	3105	3138	3091
3074	3051	3067	3043	3074	3031
3074	3051	3067	3043	3074	3031
1670	1645	1658	1632	1603	1555
1664	1639	1652	1626	1597	1551
1497	1471	1497	1471	1493	1470
1497	1470	1497	1471	1493	1470
1491	1464	1491	1462	1485	1458
1490	1463	1490	1463	1484	1457
1444	1415	1444	1416	1421	1400
1441	1413	1442	1415	1421	1399
1392	1364	1389	1361	1299	1265
1385	1356	1382	1353	1288	1256
1110	1084	1101	1076	1083	1075
1109	1078	1100	1075	1082	1075
1092	1071	1084	1073	1076	1057
1089	1070	1083	1067	1073	1048
1029	1017	1028	1016	1009	997
1028	1016	1028	1016	1007	996
963	958	967	962	913	898
958	954	962	958	907	891

(continued)

Table 2.10 (continued)

Gas		DMSO		CCl_4	
		PCM	PCM	PCM	PCM
6-31G*	6-311++G**	6-31G*	6-311++G**	6-31G*	6-311++G**
720	719	726	725	731	731
713	713	717	718	725	727
611	617	617	624	631	643
608	614	614	620	628	640
523	522	526	525	540	543
513	512	513	513	533	537
454	446	455	446	454	449
384	381	388	384	391	391
327	320	330	322	322	323
284	281	284	281	299	298
266	260	267	261	280	276
233	228	237	231	241	235
210	199	209	199	235	237
193	177	199	182	189	192
181	172	187	179	184	183
148	146	151	150	161	165
105	100	115	113	129	154
87	74	103	101	92	151
78	63	101	84	89	132
53	46	81	77	69	92
52	45	68	68	68	90

Table 2.11 Experimental frequencies (cm^{-1}) for chromyl acetate

Experimental[a]		Assignment[c]				
IR solid	IR solution	Chromyl acetate[a]	SQM[b]	Monodentate	SQM[b]	Bidentate
2965		νCH_3	2997	ν_a CH_3 ip	3057	ν_a CH_3
			2997	ν_a CH_3op	3057	ν_a CH_3
2947			2956	ν_a CH_3 ip	3016	ν_a CH_3
			2956	ν_a CH_3op	3016	ν_a CH_3
2930		νCH_3	2894	ν_s CH_3 ip	2953	ν_s CH_3
			2894	ν_s CH_3 op	2953	ν_s CH_3
1714	1660	ν_a C=O (monodentate)	1624	ν_s C=O i p	1604	ν_a COO ip
1610	1621	ν_a C=O (bridge)	1612	ν_a C=O op	1600	ν_a COO op
1540	1575		1499	δa CH_3 ip	1430	δ CH_3
			1499	δa CH_3 op	1430	δ CH_3
1453	1453	ν_a C=O (bridge)	1492	δa CH_3 ip	1425	δ CH_3
			1490	δa CH_3 op	1424	δ CH_3
	1432		1422	δs CH_3 i p	1385	ν_sCOO ip
			1421	δs CH_3 op	1380	δs CH_3
1417	1371	ν_s C=O (monodentate)	1378	ν_s C–O	1333	δs CH_3
1352		δs CH_3	1366	ν_a C–O	1326	ν_sCOO op
			1098	ρCH_3 ip	1125	ν_s Cr=O
			1097	ρCH_3 op	1122	ν_a Cr=O
1045		ρCH_3	1024	ρCH_3 ip	1041	ρCH_3
			1024	ρCH_3 op	1041	ρCH_3
	977	νCr=O	1003	ν_s Cr=O	986	ρCH_3
	945	νCr=O	995	ν_a Cr=O	986	ρCH_3
900		νC–C	953	ν_s Cr=O, δs O–Cr–O	933	νC–C
883 sh		νC–C	948	ν_a Cr=O, δa O–Cr–O	930	δCOOip
755 br			723	δCOOip, νC–C	714	ν C–C
668	677	δCOO	714	δCOOop, νC–C	704	δCOOop
655 sh			643	γCOOip	586	γCOOip
	628		642	γCOOop	583	γCOOop
619	618	ρ C–COO in-plane	508	ρCOOip	519	ρCOOip
	609		506	ρCOOop	506	ρCOOop
440	440	ρ C–COO out-plane	481	δCrO_2	438	δCrO_2
410	407		391	Wag CrO_2	376	ν_a Cr–O
			326	ν_a Cr–O	323	ν_s Cr–O
			304	ν_s Cr–O	260	δa O–Cr–O
			296	δa O–Cr–O	245	ρ CrO_2
			256	δs O–Cr–O	214	τwCrO_2
			217	δs Cr–O–C	195	νCr–O
			214	τCOOip	189	τC–O
			212	δa Cr–O–C	176	νCr–O

(continued)

Table 2.11 (continued)

Experimental[a]		Assignment[c]				
IR solid	IR solution	Chromyl acetate[a]	SQM[b]	Monodentate	SQM[b]	Bidentate
			152	δs O–Cr–O	137	δs O–Cr–O
			108	τCOOop	97	ν C ← O
			88	τC–O	81	τCOOop
			78	τC–O	71	ν C ← O
			60	$\tau w CH_3$	48	$\tau w CH_3$
			56	$\tau w CH_3$	48	$\tau w CH_3$

Abbreviations ν stretching, δ deformation, ρ rocking; *wag*, (γ) wagging, τw torsion, *a* antisymmetric, *s* symmetric, *op* out of phase, *ip* in phase

[a] Ref [8]

[b] From B3LYP/6-31G*

[c] This work

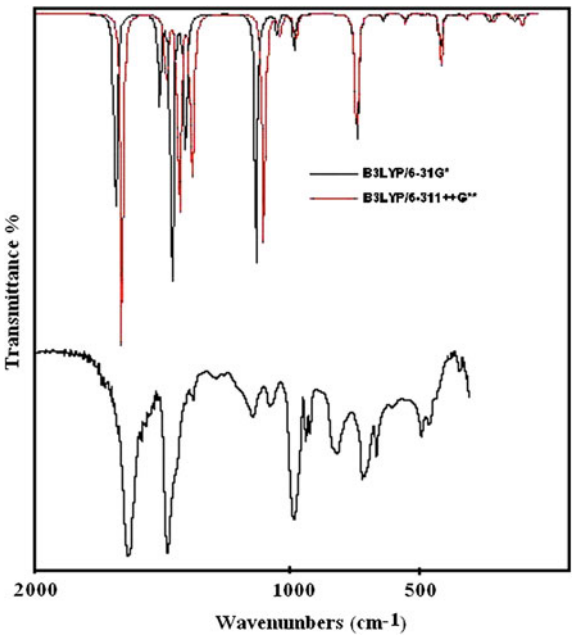

Fig. 2.2 Theoretical Infrared spectrum of $CrO_2(CH_3COOH)_2$ at B3LYP/6-31G* and B3LYP/6-311++G** theory levels (*upper*) compared with the experimental in solid phase (*bottom*)

2.6 Coordination Monodentate of the Acetate Groups

Practically all the vibration modes considering monodentate coordination of the acetate groups for chromyl acetate are perfectly characterized by the DFT/B3LYP/6-31G* and B3LYP/6-311++G** calculations and the contribution PED values almost do not change with the used method. The definition of natural internal coordinates for chromyl acetate with monodentate coordination adopted for acetate groups appear in Table 2.12.

2.7 CH_3 Modes

The IR bands at 2,965, 2,947, and 2,930 cm^{-1} are associated with the CH_3 stretchings and are calculated in all cases as pure modes. The in-phase modes have A symmetries while the out-of-phase modes have B symmetries. In the infrared spectrum of acetic acid these modes are observed at 3,051, 2,996, and 2,944 cm^{-1} [51], while in the infrared spectrum of barium acetate these modes appear at 3,128, 2,974, and 2,937 cm^{-1} [31]. The frequencies corresponding to CH_3 bending, rocking, and twisting modes are observed at expected frequencies. In the acetic acid, the CH_3 bending modes are calculated using 6-31G* basis set at 1,490, 1,484, and 1,423 cm^{-1} and observed at 1,430 and 1,382 cm^{-1} [51]. In chromyl acetate the PED values show that these modes are calculated as pure modes and for this reason they are assigned to the bands at 1,453 and 1,432 cm^{-1}. In acetic acid, the rocking modes are predicted, using a 6-31G* basis set, at 1,070 and 1,002 cm^{-1} and are observed at 1,048 and 989 cm^{-1} [51]. In chromyl acetate, these modes are calculated using 6-31G* basis set at 1,098, 1,097, 1,029, and 1,024 cm^{-1}. The modes at 1,098 and 1,029 cm^{-1} are assigned to CH_3 rocking modes in-phase while the remains are the corresponding out-of-phase modes. The CH_3 twisting modes in chromyl acetate are calculated at 60 and 56 cm^{-1} and the PED value indicate that these modes are strongly coupled with other modes but in this region with higher PED %. In acetic acid the CH_3 twisting mode is calculated using a 6-31G* basis set at 79 cm^{-1} and observed at 75 cm^{-1} [51].

2.8 Carboxylate Modes

The C = O antisymmetric and symmetric stretching modes reported in a previous paper [8] of $CrO_2(CH_3COO)_2$ solid were assigned to the strong bands observed in the infrared spectrum at 1,714 and 1,610 cm^{-1}, respectively. In acetic acid, this mode was calculated at 1,855 and observed at 1,788 cm^{-1} [51]. In this case, the two C = O stretching modes are calculated by the B3LYP/6-31G* method at 1,670 and 1,664 cm^{-1}. The frequencies predicted for these vibrational modes

Table 2.12 Definition of natural internal coordinates for chromyl acetate with monodentate coordination adopted for acetate groups

Symmetry A	
S_1 = 2s (12-15) − s (12-14) − s (12-13) + 2s (8-11) − s (8-9) − s (8-10)	νa (CH_3) ip
S_2 = s (12-13) − s (12-14) + s (8-9) − s (8-10)	νa (CH_3) ip
S_3 = s (12-15) + s (12-14) + s (12-13) + s (8-11) + s (8-9) + s (8-10)	νs (CH_3) ip
S_4 = q (16-5) + q (17-7)	νs (C=O)
S_5 = β (11-8-9) − β (11-8-10) + β (13-12-15) − β (14-12-15)	δa (CH_3) ip
S_6 = 2 β (9-8-10) − β (11-8-9) − β (11-8-10) + 2 β (14-12-13) − β (13-12-15) − β (14-12-15)	δa (CH_3) ip
S_7 = q (16-4) + q (17-6)	ν (C–O) ip
S_8 = β (9-8-10) + β (11-8-9) + β (11-8-10) − α (16-8-9) -α (16-8-10) − α (16-8-11) + β (14-12-13) + β (13-12-15) + β (14-12-15) − α (17-12-13) − α (17-12-14) − α (17-12-15)	δs (CH_3) ip
S_9 = q (1-2) + q (1-3)	νs (Cr=O)
S_{10} = α (16-8-9) − α (16-8-10) + α (17-12-13) − α (17-12-14)	ρ (CH_3) ip
S_{11} = 2α (16-8-11) − α (16-8-9) -α (16-8-10) + 2 α (17-12-15) − α (17-12-13) − α (17-12-14)	ρ (CH_3) ip
S_{12} = r (12-17) + r (8-16)	ν (C–C) ip
S_{13} = 2ψ (4-16-5) − ψ (4-16-8) − ψ (5-16-8) + 2 ψ (6-17-7) − ψ (6-17-12) − ψ (7-17-12)	δ (O=C–O) ip
S_{14} = γ (8-16-5-4) + γ (12-17-7-6)	γ (COO) ip
S_{15} = t (1-4) + q (1-6)	νs (Cr–O)
S_{16} = θ (2-1-3)	δ (CrO_2)
S_{17} = ψ (4-16-8) − ψ (5-16-8) − ψ (7-17-12) + ψ (6-17-12)	ρ (COO) ip
S_{18} = ϕ (3-1-4) − ϕ (3-1-6) + ϕ (2-1-6) − ϕ (2-1-4)	ρ (CrO_2)
S_{19} = τ (3-1-4-16) + τ (2-1-4-16) + τ (2-1-6-17) + τ (3-1-6-17)	τ (C–O) ip
S_{20} = θ (1-4-16) + θ (1-6-17)	δ (Cr–O-C) ip
S_{21} = ϕ (6-1-4)	δ (O–Cr–O)
S_{22} = τ (1-4-16-8) + τ (1-4-16-5) − τ (1-6-17-12) − τ (1-6-17-7)	τ (COO) op
S_{23} = τ (4-16-8-9) + τ (4-16-8-10) + τ (4-16-8-11) + τ (6-17-12-13) + τ (6-17-12-14) + τ (6-17-12-15)	τ (CH_3) ip
Symmetry B	
S_{24} = 2s (12-15) − s (12-14) − s (12-13) − 2s (8-11) + s (8-9) + s (8-10)	νa (CH_3) op
S_{25} = s (12-14) − s (12-13) + s (8-9) − s (8-10)	νa (CH_3) op

(continued)

Table 2.12 (continued)

S_{26} = s (12-15) + s (12-14) + s (12-13) − s (8-11) − s (8-9) − s (8-10)	νs (CH_3) op
S_{27} = q (16-5) − q (17-7)	νa (C=O) op
S_{28} = β (11-8-9) − β (11-8-10) − β (13-12-15) + β (14-12-15)	δa (CH_3) op
S_{29} = 2β (9-8-10) − β (11-8-9) − β (11-8-10) − 2 β (14-12-13) + β (13-12-15) + β (14-12-15)	δa (CH_3) op
S_{30} = q (16-4) − q (17-6)	ν (C–O) op
S_{31} = β (9-8-10) + β (11-8-9) + β (11-8-10) − α (16-8-9) -α (16-8-10) − α (16-8-11) − β (14-12-13) − β (13-12-15) − β (14-12-15) + α (17-12-13) + α (17-12-14) + α (17-12-15)	δs (CH_3) op
S_{32} = q (1-2) − q (1-3)	νa (Cr=O)
S_{33} = α (16-8-10) − α (16-8-9) + α (17-12-13) − α (17-12-14)	ρ (CH_3) op
S_{34} = 2α (16-8-11) − α (16-8-9) -α (16-8-10) − 2 α (17-12-15) + α (17-12-13) + α (17-12-14)	ρ (CH_3) op
S_{35} = r (12-17) − r (8-16)	ν (C–C) op
S_{36} = 2ψ (4-16-5) − ψ (4-16-8) − ψ (5-16-8) − 2 ψ (6-17-7) + ψ (6-17-12) + ψ (7-17-12)	δ (O=C–O) op
S_{37} = γ (8-16-5-4) − γ (12-17-7-6)	γ (COO) *o*p
S_{38} = t (1-4) − q (1-6)	νa (Cr–O)
S_{39} = ψ (4-16-8) − ψ (5-16-8) + ψ (7-17-12) − ψ (6-17-12)	ρ (COO) *o*p
S_{40} = ϕ (3-1-4) + ϕ (2-1-4) − ϕ (3-1-6) − ϕ (2-1-6)	Wag (CrO_2)
S_{41} = ϕ (3-1-4) − ϕ (2-1-4) + ϕ (3-1-6) − ϕ (2-1-6)	τ (CrO_2)
S_{42} = θ (1-4-16) − θ (1-6-17)	δ (Cr–O-C) op
S_{43} = τ (1-4-16-8) + τ (1-4-16-5) − τ (1-6-17-12) − τ (1-6-17-7)	τ (COO) ip
S_{44} = τ (3-1-4-16) + τ (2-1-4-16) − τ (2-1-6-17) − τ (3-1-6-17)	τ (C–O) ip
S_{45} = τ (4-16-8-9) + τ (4-16-8-10) + τ (4-16-8-11) + τ (6-17-12-13) + τ (6-17-12-14) + τ (6-17-12-15)	τ (CH_3) op

Abbreviations q Cr=O bond distance, t Cr–O bond distance, s = C–H bond distance, θ = O=Cr=O bond angle, ϕ = O–Cr–O bond angle, ψ = C–C–O bond angles, β = H–C–H bond angle, α, C–C–H bond angle.

Abbreviations ν stretching, δ deformation, ρ in the plane bending or rocking, γ out of plane bending or wagging, w twisting, a antisymmetric, s symmetric, *ip* in phase, *op* out of phase

show that the two stretching modes are split by about 6 cm^{-1} with the 6-31G* basis set. Both B3LYP methods underestimate the C = O stretching frequencies as compared to the experimental values. The modes are calculated as pure modes and both modes are assigned to the bands at 1,714 and 1,610 cm^{-1}, respectively, as in a previous paper [8]; moreover, the difference among them is of 9 cm^{-1}. Normally, the antisymmetric C = O stretching frequencies of the metal acetates are observed between 1,610 and 1,540 cm^{-1}, while the corresponding symmetric C = O stretching frequencies are observed among 1,451 and 1,394 cm^{-1} [12, 15, 19–22]. In the $NaCH_3COO$ compound [12] the antisymmetric C = O stretching is observed at 1,556 cm^{-1}, in $Ni(CH_3COO)_2$ compound at 1,600 cm^{-1} [12], while this vibration mode in $Cu(CH_3COO)_2$ [22] is observed at 1,610 cm^{-1}. Agambar et al. [22] have assigned the δ(COO) mode for $NaCH_3COO$ compound to the IR band at 645 cm^{-1}, while Spinner et al. [17] for the same compound have assigned the two δ(COO) in-phase modes to the Raman bands at 652 and 622 cm^{-1}, respectively. The calculations for acetic acid show the δ(COO) and wagging (COO) modes at 682 and 582 cm^{-1}, respectively, and were experimentally assigned to the bands at 657 and 642 cm^{-1}, respectively [51]. The theoretical calculations for chromyl acetate predict the two δ(COO) in-phase and out-of-phase modes at 723 and 714 cm^{-1}, respectively, whereas the corresponding wagging (COO) modes are calculated at 643 and 642 cm^{-1}. All the modes appear coupled with other modes. In chromyl acetate, the two δ(COO) modes are assigned to the bands at 755 and 678 cm^{-1}, respectively, while the two wagging (COO) modes are assigned to the shoulder and IR band at 655 and 628 cm^{-1}, respectively. The ρ(COO) in-phase and out-of-phase modes for chromyl acetate could be assigned to the bands at 619 and 609 cm^{-1}. Both modes have different symmetries and appear slightly coupled with other modes as the PED values predict. In acetic acid compound the twisting (COO) mode is calculated at 419 cm^{-1} and experimentally observed at 565 cm^{-1} [51], while this mode for $NaCH_3COO$ was assigned by Spinner et al. [17] at 247 cm^{-1}. In a previous paper of chromyl acetate this mode was not assigned but, in this case the theoretical calculations predict the two twisting (COO) in-phase and out-of-phase modes at 214 and 108 cm^{-1}, respectively. In this low region in the Raman spectrum of numerous compounds that contain carboxylate groups, such $NaCH_3COO$, $Ba(CH_3COO)_2$ [31], and benzoic acid compounds [67, 68], it is possible to observe many bands with higher intensity probably due to additional resonance interactions. In the benzoic acid, Florio et al. [67] have observed them as a consequence of the fact that normal mode OH bend vibrations of cyclic dimer have contributions from both the OH and CH bends. This leads to a sharing of intensities over many states, which fills in the lower frequency region of the spectrum for benzoic acid dimer. Another cause would be as observed by Reva et al. [68] in the same cyclic dimer that the other more strongly H-bonded dimer may have more substantial contributions from the coupling of the OH stretch with the intermolecular stretch.

2.9 Chromyl Modes

In chromyl nitrate the unscaled DFT frequencies for the symmetric Cr=O stretchings mode are higher than the frequencies of the antisymmetric Cr=O stretchings [9, 10]. In this compound these modes are uncoupled with other modes. In other chromyl compounds these modes appear in 1,050–900 cm^{-1} region, i.e., in $CrO_2(ClO_4)_2$ they appear at 990 and 980 cm^{-1} [68], in $CrO_2(SO_3F)_2$ appear at 1,061 and 1,020 cm^{-1} [70], and in CrO_2F_2 and CrO_2Cl_2 they are observed for the first compound at 1,016 and 1,006 cm^{-1} while for the second one at 1,002 and 995 cm^{-1} respectively [70, 71]. The predicted frequencies for the vibrational modes of chromyl acetate show that the antisymmetric and symmetric Cr=O stretchings are slightly split indicating a small contribution of the central Cr atom in these vibrations. In this compound, the symmetric Cr=O stretching mode was also calculated at higher frequency (1,003 cm^{-1}) than the corresponding antisymmetric mode (995 cm^{-1}). The intensities of these bands using 6-31G* and 6-311++G** basis sets are not predicted correctly because the more intense band is related to the antisymmetric mode as it was observed in chromyl nitrate [10]. Previously, the two modes were assigned to the band observed in the infrared spectrum of the solid compound at 948 cm^{-1} [9]. In this case both modes are assigned to the IR bands observed in the spectrum of the sample in solution at 977 and 945 cm^{-1}.

The theoretical antisymmetric and symmetric Cr–O stretching modes in $CrO_2(ClO_4)_2$ are observed, respectively, at 380 and 355 cm^{-1} [68] and in $CrO_2(NO_3)_2$ they were assigned these modes at 460 and 446 cm^{-1}, respectively [9, 10]. In this case the theoretical calculation predicts the antisymmetric and symmetric Cr–O stretching modes at 326 and 304 cm^{-1}, in form similar to that observed in chromyl nitrate [10].

The CrO_2 bending mode is observed in CrO_2F_2 at 364 cm^{-1} while in CrO_2Cl_2 it is observed at 356 cm^{-1} [71, 72]. In this chapter, the B3LYP/6-31G* method calculates the CrO_2 bending at 481 cm^{-1} in form similar to chromyl nitrate (453 cm^{-1}) [10]. With the other basis set this mode appears also coupled. Here, the IR band at 440 cm^{-1} was assigned to the CrO_2 bending. The other O–Cr–O bending modes are calculated at 296 and 256 cm^{-1} with 6-31G* basis set.

The wagging, rocking, and twisting modes of the CrO_2 group are not assigned in a previous paper [9]. In this case the calculations predict these modes in the low frequencies region and all modes are coupled with other modes of the acetate groups. The wagging CrO_2 mode is calculated using 6-31G* basis set at higher frequency (391 cm^{-1}) and with higher contribution PED than the rocking mode (296 cm^{-1}).

The CrO_2 twisting mode was not assigned previously. The PED values indicate that this mode is strongly coupled with vibrations of the same group and the acetate group. In this case this mode could be assigned at 256 cm^{-1} because it appears with a higher PED value.

2.10 Coordination Bidentate of the Acetate Groups

2.10.1 Acetate Groups as Rings of Four Members

In this case we performed calculations with the two basis sets considering both acetate groups as a ring of four members where the deformations and torsion coordinates of these groups have been defined as proposed by Fogarasi et al. [39] and are observed in Table 2.13. In this case a notable change in the assignment, in relation to the above monodentate considerations, is observed.

2.10.2 CH_3 Modes

In this case, a CH_3 bending mode is predicted at 1,333 cm^{-1}, while two CH_3 rocking modes are calculated at 986 cm^{-1} different from the monodentate coordination, as observed in Table 2.11 The twisting modes are observed at expected frequencies and calculated at 48 cm^{-1}.

2.10.3 Acetate Group

For this group, the more significant difference in relation to the monodentate case is presented. In this case, a C–O symmetric stretching in-phase mode is clearly predicted at 1,385 cm^{-1}, while one of the two δ(COO) modes is calculated at 930 cm^{-1} in reference to the above monodentate type, as shown in Table 2.11 The expected C ← O antisymmetric and symmetric modes are calculated at 97 and 71 cm^{-1}, while one of the two twisting (COO) modes is clearly calculated at 81 cm^{-1}.

2.10.4 Chromyl Group

For this group the calculations predict the two Cr=O stretchings at frequencies different from the monodentate case, the antisymmetric Cr=O stretchings are calculated at 1,122 cm^{-1}, while the corresponding symmetric stretchings are at 1,125 cm^{-1}.

The CrO_2 bending and the remains modes of this group are observed at practically the same frequencies as the above monodentate coordination.

For this analysis we think that the monodentate coordination is possible for this compound because the two Cr=O stretching modes should be observed with

Table 2.13 Definition of natural internal coordinates for chromyl acetate with bidentate coordination adopted for acetate groups

Symmetry A	
$S_1 = 2s\ (12\text{-}15) - s\ (12\text{-}14) - s\ (12\text{-}13) + 2s\ (8\text{-}11) - s\ (8\text{-}9) - s\ (8\text{-}10)$	νa (CH_3) ip
$S_2 = s\ (12\text{-}13) - s\ (12\text{-}14) + s\ (8\text{-}9) - s\ (8\text{-}10)$	νa (CH_3) ip
$S_3 = s\ (12\text{-}15) + s\ (12\text{-}14) + s\ (12\text{-}13) + s\ (8\text{-}11) + s\ (8\text{-}9) + s\ (8\text{-}10)$	νs (CH_3) ip
$S_4 = q\ (16\text{-}5) - q\ (16\text{-}4) + q\ (17\text{-}6) - q\ (17\text{-}7)$	νa (C–O) ip
$S_5 = \beta\ (11\text{-}8\text{-}9) - \beta\ (11\text{-}8\text{-}10) + \beta\ (13\text{-}12\text{-}15) - \beta\ (14\text{-}12\text{-}15)$	δa (CH_3) ip
$S_6 = 2\beta\ (9\text{-}8\text{-}10) - \beta\ (11\text{-}8\text{-}9) - \beta\ (11\text{-}8\text{-}10) + 2\ \beta\ (14\text{-}12\text{-}13) - \beta\ (13\text{-}12\text{-}15) - \beta\ (14\text{-}12\text{-}15)$	δa (CH_3) ip
$S_7 = q\ (16\text{-}5) + q\ (16\text{-}4) + q\ (17\text{-}6) + q\ (17\text{-}7)$	νs (C–O) ip
$S_8 = \beta\ (9\text{-}8\text{-}10) + \beta\ (11\text{-}8\text{-}9) + \beta\ (11\text{-}8\text{-}10) - \alpha\ (16\text{-}8\text{-}9)$ -$\alpha\ (16\text{-}8\text{-}10) - \alpha\ (16\text{-}8\text{-}11) + \beta\ (14\text{-}12\text{-}13) + \beta\ (13\text{-}12\text{-}15) + \beta\ (14\text{-}12\text{-}15) - \alpha\ (17\text{-}12\text{-}13) - \alpha\ (17\text{-}12\text{-}14) - \alpha\ (17\text{-}12\text{-}15)$	δs (CH_3) ip
$S_9 = q\ (1\text{-}2) + q\ (1\text{-}3)$	νs (Cr=O)
$S_{10} = \alpha\ (16\text{-}8\text{-}9) - \alpha\ (16\text{-}8\text{-}10) + \alpha\ (17\text{-}12\text{-}13) - \alpha\ (17\text{-}12\text{-}14)$	ρ (CH_3) ip
$S_{11} = 2\ \alpha\ (16\text{-}8\text{-}11) - \alpha\ (16\text{-}8\text{-}9)$ -$\alpha\ (16\text{-}8\text{-}10) + 2\ \alpha\ (17\text{-}12\text{-}15) - \alpha\ (17\text{-}12\text{-}13) - \alpha\ (17\text{-}12\text{-}14)$	ρ (CH_3) ip
$S_{12} = r\ (12\text{-}17) - r\ (8\text{-}16)$	ν (C–C) op
$S_{13} = r\ (12\text{-}17) + r\ (8\text{-}16)$	ν (C–C) ip
$S_{14} = \tau\ (5\text{-}1\text{-}4\text{-}16) + \tau\ (4\text{-}16\text{-}5\text{-}1) - \tau\ (1\text{-}4\text{-}16\text{-}5) - \tau\ (16\text{-}5\text{-}1\text{-}4) + \tau\ (7\text{-}1\text{-}6\text{-}17) + \tau\ (6\text{-}17\text{-}7\text{-}1) - \tau\ (1\text{-}6\text{-}17\text{-}7) - \tau\ (17\text{-}7\text{-}1\text{-}6)$	τ (COO) ip
$S_{15} = \psi\ (4\text{-}16\text{-}8) - \psi\ (5\text{-}16\text{-}8) - \psi\ (7\text{-}17\text{-}12) + \psi\ (6\text{-}17\text{-}12)$	ρ (COO) ip
$S_{16} = \phi\ (2\text{-}1\text{-}3)$	δ (CrO_2)
$S_{17} = t\ (1\text{-}4) + t\ (1\text{-}6) + t\ (1\text{-}5) + t\ (1\text{-}7)$	νs (Cr–O)
$S_{18} = \phi\ (3\text{-}1\text{-}4) - \phi\ (3\text{-}1\text{-}6) + \phi\ (2\text{-}1\text{-}6) - \phi\ (2\text{-}1\text{-}4)$	ρ (CrO_2)
$S_{19} = t\ (1\text{-}4) + t\ (1\text{-}6) - t\ (1\text{-}5) - t\ (1\text{-}7)$	νa (Cr–O)
$S_{20} = \tau\ (3\text{-}1\text{-}4\text{-}16) + \tau\ (2\text{-}1\text{-}4\text{-}16) + \tau\ (2\text{-}1\text{-}6\text{-}17) + \tau\ (3\text{-}1\text{-}6\text{-}17) + + \tau\ (2\text{-}1\text{-}7\text{-}17) + \tau\ (3\text{-}1\text{-}4\text{-}17) + \tau\ (2\text{-}1\text{-}5\text{-}16) + + \tau\ (3\text{-}1\text{-}5\text{-}16)$	τ (C–C)
$S_{21} = \phi\ (1\text{-}4\text{-}16) + \phi\ (1\text{-}6\text{-}17)$	δ (Cr–O-C) ip
$S_{22} = q\ (16\text{-}5) + q\ (16\text{-}4) - q\ (17\text{-}6) - q\ (17\text{-}5)$	νs (C–O) op
$S_{23} = \tau\ (4\text{-}16\text{-}8\text{-}9) + \tau\ (4\text{-}16\text{-}8\text{-}10) + \tau\ (4\text{-}16\text{-}8\text{-}11) - \tau\ (6\text{-}17\text{-}12\text{-}13) - \tau\ (6\text{-}17\text{-}12\text{-}14) - \tau\ (6\text{-}17\text{-}12\text{-}15)$	τ (CH_3) op

(continued)

Table 2.13 (continued)

Symmetry B	
S_{24} = 2s (12-15) − s (12-14) − s (12-13) − 2s (8-11) + s (8-9) + s (8-10)	*v*a (CH_3) op
S_{25} = s (12-14) − s (12-13) + s (8-9) − s (8-10)	*v*a (CH_3) op
S_{26} = s (12-15) + s (12-14) + s (12-13) − s (8-11) − s (8-9) − s (8-10)	*v*s (CH_3) op
S_{27} = q (16-4) − q (16-4) − q (17-6) +- q (17-7)	*v*a (C–O) op
S_{28} = β (11-8-9) − β (11-8-10) − β (13-12-15) + β (14-12-15)	δa (CH_3) op
S_{29} = 2 β (9-8-10) − β (11-8-9) − β (11-8-10) − 2 β (14-12-13) + β (13-12-15) + β (14-12-15)	δa (CH_3) op
S_{30} = β (9-8-10) + β (11-8-9) + β (11-8-10) − α (16-8-9) -α (16-8-10) − α (16-8-11) − β (14-12-13) − β (13-12-15) − β (14-12-15) + α (17-12-13) + α (17-12-14) + α (17-12-15)	δs (CH_3) op
S_{31} = q (16-5) + q (16-4) − q (17-6) − q (17-5)	*v*s (C–O) op
S_{32} = q (1-2) − q (1-3)	*v*a (Cr=O)
S_{33} = α (16-8-10) − α (16-8-9) + α (17-12-13) − α (17-12-14)	ρ (CH_3) op
S_{34} = 2 α (16-8-11) − α (16-8-9) -α (16-8-10) − 2 α (17-12-15) + α (17-12-13) + α (17-12-14)	ρ (CH_3) op
S_{35} = η (4-1-5) + η (4-16-5) − η (1-7-17) − η (1-6-17) − η (1-4-16) − η (1-5-16) + η (6-1-7) + η (6-17-7)	δ (O=C–O) ip
S_{36} = η (4-1-5) + η (4-16-5) + η (1-7-17) + η (1-6-17) − η (1-4-16) − η (1-5-16) + η (6-1-7) + η (6-17-7)	δ (O=C–O) op
S_{37} = γ (8-16-5-4) − γ (12-17-7-6)	γ (COO) *o*p
S_{38} = ψ (4-16-8) − ψ (5-16-8) + ψ (7-17-12) − ψ (6-17-12)	ρ (COO) *o*p
S_{39} = t (1-6) + t (1-7) − t (1-4) − t (1-5)	*v*a (Cr–O)
S_{40} = ϕ (2-1-7) + ϕ (2-1-6) + ϕ (3-1-7) + ϕ (3-1-6) − ϕ (2-1-4) − ϕ (2-1-5)- ϕ (3-1-4) − ϕ (3-1-5)	Wag (CrO_2)
S_{41} = ϕ (3-1-4) − ϕ (2-1-5) + ϕ (3-1-7) − ϕ (2-1-6)	τ (CrO_2)
S_{42} = t (1-6) − t (1-7) − t (1-4) + t (1-5)	*v*a (Cr–O)
S_{43} = ϕ (7-1-4) − ϕ (6-1-5)	δa (O–Cr–O)
S_{44} = τ (5-1-4-16) + τ (4-16-5-1) − τ (1-4-16-5) − τ (16-5-1-4) − τ (7-1-6-17) − τ (6-17-7-1) + τ (1-6-17-7) +- τ (17-7-1-6)	τ (COO) op
S_{45} = τ (4-16-8-9) + τ (4-16-8-10) + τ (4-16-8-11) + τ (6-17-12-13) + τ (6-17-12-14) + τ (6-17-12-15)	τ (CH_3) ip

* as two rings of four members

q = Cr=O bond distance, r = Cr–O bond distance, s = N–O bond distance, θ = O=Cr=O bond angle, ϕ = O–Cr–O bond angle, ψ = O=Cr–O bond angles, β = O–N–O bond angle

Abbreviations *v* stretching, δ deformation, ρ in the plane bending or rocking, γ out of plane bending or wagging, τw twisting, *a* antisymmetric, *s* symmetric, *ip* in phase,*op* out of phase

Table 2.14 Comparison of scaled internal force constants for chromyl acetate

	[A]Chromyl acetate			
	Monodentate		[#]Bidentate	
Coordinates	6-31G*	6-311++G**	6-31G*	6-311++G**
f (C = O)	10.38	10.38	12.19	11.94
f (C–O)	6.85	6.52	–	–
f (Cr = O)	9.09/(6.55)	8.63/(6.56)	9.09/(6.57)	8.63/(6.56)
f (Cr–O)	2.79/(6.09)	2.69/(7.34)	2.69/(1.38)	2.61/(1.27)
f (C–H)	4.99	4.92	4.99	4.92
f (C–C)	4.31	4.27	4.31	4.27
f (O = C–O)	1.66	1.57/0.93	2.12	–
f (O = Cr = O)	1.59/(2.53)	1.54/(2.26)	2.19/(1.62)	2.11/(1.63)
f (O–Cr–O)	1.00/(0.80)	0.94(0.74)	7.28/(0.65)	7.34/(0.66)
f (C–O–Cr)	1.85	1.51	–	–
f (H–C–H)	0.60	0.58	0.60	0.58
f (C = O)/(C–O)	1.76	1.81	4.67	4.62
f (C = O)/(Cr–O)	0.18	0.19	−1.78	−1.79
f (Cr–O)/(C–O)	0.84	0.78	−3.20	−3.22

Units are mdyn $Å^{-1}$ for stretching and stretching–stretching interaction and mdyn Å rad^{-2} for angle deformations

[a] This work

Among parenthesis the force constants for chromyl nitrate [12]

higher intensity at 977 and 945 cm^{-1}. The two observed strong IR bands in that region justify the stretching modes.

2.11 Force Field

The SQM force field [35–37] was obtained using the transferable scale factors of Rauhut and Pulay [36] for the acetate group and with the MOLVIB program [32, 33]. For the chromyl group the scale factors used taken were of the chromyl nitrate [5]. The corresponding force constants were estimated using the scaling procedure of Pulay et al. [28], as mentioned before. The harmonic force fields in Cartesian coordinates were transformed into the local symmetry or "natural" coordinates proposed by Fogarasi et al. [31]. The calculated force constants for both coordination modes of the acetate groups are collected in Table 2.14.

The obtained force constant values for the two considered cases could indicate the presence of both coordination modes, but the biggest obtained value in the f (O–Cr–O) force constant would indicate that the existence of the coordination bidentate for chromyl acetate is impossible.

2.12 Conclusions

In this chapter an approximate normal coordinate analysis, considering the mode of coordination adopted by acetate groups as monodentate and bidentate, was proposed for chromyl acetate.

The assignments previously made [8] were corrected and completed in accordance with the present theoretical results. The assignments of the 45 normal modes of vibration corresponding to chromyl acetate are reported.

The NBO and AIM analyses show practically a monodentate coordination of the acetate groups in chromyl acetate and a probable ionic nature of the compound.

The 6-31G * and 6-311+G basis sets at the B3LYP level were employed to obtain the molecular force fields and the vibrational frequencies.

Acknowledgments This work was subsidized with grants from CIUNT (Consejo de Investigaciones, Universidad Nacional de Tucumán). The author thanks Prof. Tom Sundius for his permission to use MOLVIB.

References

1. M. Sowinska, A. Bartecki, Transition Met. Chem. **10**(2), 63–66 (1985)
2. M. Sowinska, J. Myrczek, A. Bartecki, Spectrosc. lett. **26**(7), 1295–1309 (1993)
3. F. Freeman, P.J. Cameron, R.H. DuBois, J. Org. Chem. **33**, 3970 (1968)
4. F. Freeman, R.H. DuBois, N.J. Yamachika, Tetrahedron **25**, 3441 (1969)
5. E.J. Parish, N. Aksara, T.L. Boos, E.S. Kaneshiro, J. Chem. Res. (S), 708–709 (1999)
6. J.R. Hanson, Nat. Prod. Rep. **18**, 282–290 (2001)
7. C. Szántay, Pure Appl. Chem. **62**(7), 1299–1302 (1990)
8. S.A. Brandán, A. Ben Altabef, E.L. Varetti, J. Argent. Chem. Soc. **87**(1/2), 89–96 (1999)
9. E.L. Varetti, S.A. Brandán, A. Ben Altabef, Vib. Spectrosc. **5**, 219 (1993)
10. S.A. Brandán, M.L. Roldán, C. Socolsky, A. Ben Altabef, Spectrochim. Acta, 66A (2007)
11. C.J. Marsden, K. Hedberg, M.M. Ludwig, G.L. Gard, Inorg. Chem. **30**, 4761 (1991)
12. D.A. Edwards, R.N. Hayward, Can. J. Chem. **46**, 3443–3446 (1968)
13. S.D. Robinson, M.F. Uttley, J. Chem. Soc. Dalton. **18**, 1912–1920 (1973)
14. A.R. Katritzky, J.M. Lagowski, J.A.T. Beard, Spectrochim. Acta **16**, 964–978 (1960)
15. G.B. Deacon, R.J. Phillips, Coord. Chem. Rev. **33**, 227–250 (1980)
16. F. Vratny, C.N.R. Rao, M. Dilling, Anal. Chem. **33**, 1455 (1961)
17. E. Spinner, J. Chem. Soc. **812**, 4217–4226 (1964)
18. K. Nakamoto, C. Udovich, J. Takemoto, J. Am. Chem. Soc. **92**, 3973 (1970)
19. C.D. Garner, R.G. Senior, T.J. King, J. Am. Chem. Soc. **98**(12), 3526–3529 (1970)
20. T.A. Stephenson, S.M. Morehouse, A.R. Powell, J.P. Heffer, G. Wilkinson, J. Chem. Soc. **667**, 3632–3640 (1965)
21. T.A. Stephenson, G. Wilkinson, J. Inorg. Nucl. Chem. **29**, 2122–2123 (1967)
22. C.A. Agambar, K.G. Orrell, J. Am. Chem. Soc. A, 897–904 (1969)
23. S.Z. Haider, M.H. Khungkar, K. De, J. Inorg. Nucl. Chem. **24**, 847–850 (1962)
24. H.L. Krauss, Angew. Chem. **70**, 502 (1958)
25. M.L. Roldán, S.A. Brandán, E.L. Varetti, A. Ben Altabef, Z. Anorg, Allg. Chem. **632**, 2495 (2006)
26. S. Bell, T.J. Dines, J. Phys. Chem. A **104**, 11403 (2000)
27. A.E. Reed, L.A. Curtiss, F. Weinhold, Chem. Rev. **88**, 899 (1988)
28. J.P. Foster, F. Weinhold, J. Am. Chem. Soc. **102**, 7211 (1980)

29. A.E. Reed, F. Weinhold, J. Chem. Phys. **83**, 1736 (1985)
30. R.F.W. Bader, *Atoms in Molecules. A Quantum Theory* (Oxford University Press, Oxford, 1990). ISBN 0198558651
31. Spectral Database for Organic Compounds SDBS, IR (S.Kinugasa, K.Tanabe and T.Tamura) Raman (K.Tanabe and J.Hiraishi)
32. Gaussian 03, Revision B.01, M. J. Frisch, J. A. Pople, Gaussian, Inc., Pittsburgh PA, 2003
33. A.B. Nielsen, A.J. Holder, *GaussView, User′s Reference*, (Gaussian, Inc., Pittsburgh, 1997–1998)
34. A.D. Becke, J. Chem. Phys. **98**, 5648 (1993)
35. C. Lee, W. Yang, R.G. Parr, Phys. Rev., B **37**, 785 (1988)
36. P. Pulay, G. Fogarasi, F. Pang, J.E. Boggs, J. Am. Chem. Soc. **101**(10), 2550 (1979)
37. T. Sundius, J. Mol. Struct. **218**, 321 (1990)
38. T. Sundius, *MOLVIB: A Program for Harmonic Force Field Calculation*, QCPE Program No. 604, (1991)
39. G. Fogarasi, P. Pulay, In: Vibrational spectra and structure, Vol. 14, J. E. Durig (Ed.), (Elsevier, Amsterdam, 125) 1985
40. P. Pulay, G. Fogarasi, G. Pongor, J.E. Boggs, A. Vargha, J. Am. Chem. Soc. **105**, 7037 (1983)
41. G. Rauhut, P. Pulay, J. Phys. Chem. **99**, 3093 (1995)
42. G. Rauhut, P. Pulay, J. Phys. Chem. **99**, 14572 (1995)
43. E.D. Glendening, A.E. Reed, J.E. Carpenter, F. Weinhold, NBO Version 3.1
44. AIM 2000 designed by, University of Applied Sciences, Bielefeld, Germany
45. O. Tapia, J. Chim. Phys. **87**, 875 (1990)
46. S.A. Brandán, S.B. Díaz, R. Cobos Picot, E.A. Disalvo, A. Ben Altabef, Spectrochim. Acta. **66**, 1152–1164 (2007)
47. C.C. Pye, W.W. Rudolph, J. Phys. Chem. A **107**, 8746 (2003)
48. J. Tomasi, M. Persico, Chem. Rev. **94**, 2027 (1994)
49. J. Tomasi, in: C.J. Cramer, D.G. Truhlar (Eds.), (Am. Chem. Soc., Washington, 1994), 10
50. S. Miertus, E. Scrocco, J. Tomasi, Chem. Phys. **55**, 117 (1981)
51. M. Ibrahim, E. Koglin, Acta Chim. Slov. **51**, 453–460 (2004)
52. W.H. Zachariasen, H.A. Plettinger, Acta Cryst. **12**, 526–530 (1959)
53. J.N. Van Niekerk, F.R.L. Schoening, J.F. De Wet, Acta Cryst. **6**, 501–504 (1953)
54. L.Y. Hsu, C.E. Nordman, Acta Cryst. C **39**, 690–694 (1983)
55. I. Gautier-Luneau, A. Mosset, J. Solid State Chem. **73**(2), 473–479 (1988)
56. R.J. Gillespie (ed.), *Molecular Geometry* (Van Nostrand-Reinhold, London, 1972)
57. R.J. Gillespie, I. Bytheway, T.H. Tang, R.F.W. Bader, Inorg. Chem. **35**, 3954 (1996)
58. M. Fernández Gómez, A. Navarro, S.A. Brandán, C. Socolsky, A. Ben Altabef, E.L. Varetti, J. Mol. Struct. (THEOCHEM) **626**, 101 (2003)
59. S. Wojtulewski, S.J. Grabowski, J. Mol. Struct. **621**, 285 (2003)
60. S.J. Grabowski, Monat. für Chem. **133**, 1373 (2002)
61. R.F.W. Bader, J. Phys. Chem. A **102**, 7314 (1998)
62. P.L.A. Popelier, J. Phys. Chem. A **102**, 1873 (1998)
63. U. Koch, P.L.A. Popelier, J. Phys. Chem. **99**, 9747 (1995)
64. G.L. Sosa, N. Peruchena, R.H. Contreras, E.A. Castro, J. Mol. Struct. (THEOCHEM) **401**, 77 (1997)
65. G.L. Sosa, N. Peruchena, R.H. Contreras, E.A. Castro, J. Mol. Struct. (THEOCHEM) **577**, 219 (2002)
66. G. M. Florio, T.S. Zwier, E.M. Myshakin, K.D. Jordan, E.L. Sibert, J. Chem. Phys., **118**(4) (2003)
67. I.D. Reva, S.G. Stepanian, J. Mol. Struc. **349**, 337–340 (1995)
68. M. Chaabouni, T. Chausse, J.L. Pascal, J. Potier, J. Chem. Research **5**, 72 (1980)
69. S.D. Brown, G.L. Gard, Inorg. Chem. **12**, 483 (1973)
70. H. Siebert, "*Anwendungen der schwingungsspektroskopie in der Anorganische Chemie*", (Springer, Berlin, 1966), 72
71. K. Nakamoto, Infrared and Raman Spectra of Inorganic and Coordination Compounds, 5° Ed., J. Wiley & Sons, Inc., New York, 1997